

UNIVERSITY OF OKLAHOMA

GRADUATE COLLEGE

MATERIAL ANALYSIS FOR HIGH-EFFICIENCY POLYMER COMPOSITE HEAT
EXCHANGER

A THESIS

SUBMITTED TO THE GRADUATE FACULTY

in partial fulfillment of the requirements for the

Degree of

MASTER OF SCIENCE IN MECHANICAL ENGINEERING

By

LEJLA ŠIŠIĆ

Norman, Oklahoma

2020

MATERIAL ANALYSIS FOR HIGH-EFFICIENCY POLYMER COMPOSITE HEAT
EXCHANGER

A THESIS APPROVED FOR THE
SCHOOL OF AEROSPACE AND MECHANICAL ENGINEERING

BY THE COMMITTEE CONSISTING OF

Dr. M. Cengiz Altan, Chair

Dr. Mrinal C. Saha

Dr. Yingtao Liu

© Copyright by LEJLA ŠIŠIĆ 2020

All Rights Reserved

I would like to dedicate this work to my family- thank you for always supporting me and believing in me.

Acknowledgements

I gratefully acknowledge the financial support received from the Oak Ridge National Laboratory to conduct this research.

I would like to express my deepest gratitude to my advisor, Dr. M. Cengiz Altan, for sharing his extensive knowledge and work ethics with me. His continuous guidance and support throughout my graduate studies helped me to complete this research in difficult times filled with many uncertainties. I would also like to thank Dr. Mrinal C. Saha and Dr. Yingtao Liu for sharing their excellent suggestions as my committee members.

Dr. Gorkem E. Guloglu, Dr. Maya Pishvar, and Dr. Mehrad Amirkhosravi- thank you for your invaluable assistance throughout this study. Furthermore, I wish to thank all the AME faculty and staff members for their help and availability, especially Bethany Burklund.

A special thank you goes to my family and friends for their endless motivation, encouragement, and love.

Table of Contents

Acknowledgements	v
Table of Contents	vi
List of Tables	viii
List of Figures	ix
Abstract	xiii
Chapter I: Introduction.....	1
1. Topic background.....	1
2. Literature review	2
2.1 Polymer heat exchangers.....	2
2.2 Improving thermal conductivity in polymer heat exchangers.....	6
3. Topic scope and proposed research	9
Chapter II: High Thermal Conductivity Composite Material	11
1. Objective	11
2. Materials	11
2.1 Commercially available materials	11
2.2 Composite materials prepared in the laboratory	14
3. Fabrication methods	18
4. Characterization methods	23
4.1 Density, thermal, and mechanical properties	23
4.2 Microstructure morphology.....	24
5. Characterization results for the materials	24
5.1 Thermal properties measurements.....	24
5.2 Microstructure morphology of the composite laminates	32
5.3 Mechanical properties of the composite laminates	48

Chapter III: Design and 3D Printing of the Heat Exchanger and Flow Channels	50
1. Objective	50
2. Compact heat exchanger design	50
2.1 3D model of the compact heat exchanger	50
2.2 3D model of the heat exchanger flow channels.....	54
3. 3D printing of the heat exchanger and flow channels models	57
Chapter IV: Fabrication of the Compact Polymer Heat Exchanger	60
1. Objective	60
2. Materials	61
3. Fabrication of expandable flow channels	63
3.1 Fabrication of the flow channels silicone molds	63
3.2 Fabrication of expandable flow channels	63
4. Fabrication of the compact polymer heat exchanger	65
4.1 Fabrication of the heat exchanger silicone molds	65
4.2 Fabrication of the compact polymer heat exchanger	66
4.2.1 Neat epoxy heat exchanger	66
Chapter V: Concluding remarks	70
1. Results and conclusion	70
2. Future work recommendation	72
References	73

List of Tables

Table 1: Different weight and volume percentage of graphite-graphene hybrid	5
Table 2: Freeman products that may be suitable for heat exchanger applications	12
Table 3: Selected material candidate from Freeman products for heat exchanger applications....	13
Table 4: Selected material candidate from Epoxies products for heat exchanger applications....	13
Table 5: Freeman vs. Epoxies resin properties based on the data from the supplier	14
Table 6: Epoxy properties from the material data	14
Table 7: Sigma-Aldrich, Co. copper powder	15
Table 8: Summary of Freeman laminate testing results.....	26
Table 9: Summary of Epoxies laminate testing results	27
Table 10: Summary of neat epoxy EPIKOTE™ RIMR 135+RIMH 137 laminate testing results.....	29
Table 11: Thermal conductivity values for different laminates.....	31
Table 12: Summary of graphite laminates flexural test results	48
Table 13: Properties of ABS	58
Table 14: Properties of AeroMarine silicone product	61

List of Figures

Figure 1: Plate and fin air conditioning heat exchanger	1
Figure 2: SEM image of the copper powder as received (Sigma-Aldrich).....	16
Figure 3: SEM image of Asbury Carbons graphite flakes	17
Figure 4: SEM image of Asbury Carbons graphene nano powder	18
Figure 5: Freeman laminate (bottom and top)	19
Figure 6: Epoxies laminate (bottom and top)	19
Figure 7: 20% Cu/ EPIKOTE™ RIMR 135+RIMH 137 laminate (bottom and top	20
Figure 8: 600% Cu/ EPIKOTE™ RIMR 135+RIMH 137 laminate (bottom and top).....	20
Figure 9: Fisher Scientific Thermo oven	21
Figure 10: 35% graphite/ RIMR 135 + RIMH 137 laminate fabricated using methods (i) and (vii).....	22
Figure 11: Freeman laminate (TGA test).....	25
Figure 12: Freeman laminate (DMA test).....	25
Figure 13: Epoxies laminate (TGA test).....	26
Figure 14: Epoxies laminate (DMA test).....	27
Figure 15: Neat epoxy EPIKOTE™ RIMR 135+RIMH 137 laminate (TGA test).....	28
Figure 16: Neat epoxy EPIKOTE™ RIMR 135+RIMH 137 laminate (DMA test).....	28
Figure 17: 20% Cu/ RIMR 135+RIMH 137 laminate (TGA test).....	29
Figure 18: 20% Cu/ RIMR 135+RIMH 137 laminate (DMA test).....	30
Figure 19: 300% Cu/ RIMR 135+RIMH 137 laminate (TGA test).....	30
Figure 20: 300% Cu/ RIMR 135+RIMH 137 laminate (DMA test).....	31
Figure 21: a) Freeman laminate SEM (1), b) Freeman laminate SEM (2)	32

Figure 22 a) Epoxies laminate SEM (1), b) Epoxies laminate SEM (2)	33
Figure 23: a) 20% Cu/ RIMR 135 + RIMH 137 SEM (1), b) 20% Cu/ RIMR 135 + RIMH 137 SEM (2)	34
Figure 24: 300% Cu/ RIMR 135 + RIMH 137 SEM (1), b) 20% Cu/ RIMR 135 + RIMH 137 SEM (2)	35
Figure 25: a) 500% Cu/ RIMR 135 + RIMH 137 SEM (1), b) 500% / RIMR 135 + RIMH 137 SEM (2)	36
Figure 26 a) 600% Cu/ RIMR 135 + RIMH 137 SEM (1), b) 600% / RIMR 135 + RIMH 137 SEM (2)	37
Figure 27: a) 7% graphite/ RIMR 135 + RIMH 137 at x500.....	38
Figure 27: b) 14% graphite/ RIMR 135 + RIMH 137 at x500	39
Figure 28: a) 7% graphite/ RIMR 135 + RIMH 137 at x2,500.....	39
Figure 28: b) 14% graphite/ RIMR 135 + RIMH 137 at x2,500	40
Figure 29: a) 7% graphite/ RIMR 135 + RIMH 137 at x10,000.....	40
Figure 29: b) 14% graphite/ RIMR 135 + RIMH 137 at x10,000	41
Figure 30: a) 20% graphite/ RIMR 135 + RIMH 137 at x50, b) 35% graphite/ RIMR 135 + RIMH 137 at x100	42
Figure 31: a) 20% graphite/ RIMR 135 + RIMH 137 at x1,500, b) 35% graphite/ RIMR 135 + RIMH 137 at x1,500	43
Figure 32: a) 20% graphite/ RIMR 135 + RIMH 137 at x10,000, b) 35% graphite/ RIMR 135 + RIMH 137 at x10,000	44
Figure 33: a) 15+5% graphite/ RIMR 135 + RIMH 137 at x100, b) 30+5% graphite/ RIMR 135 + RIMH 137 at x100	45
Figure 34: a) 15+5% graphite/ RIMR 135 + RIMH 137 at x2,500, b) 30+5% graphite/ RIMR 135 + RIMH 137 at x2,500	46

Figure 35: a) 15+5% graphite/ RIMR 135 + RIMH 137 at x10,000, b) 30+5% graphite/ RIMR 135 + RIMH 137 at x10,000.....	47
Figure 36: 3D model of the compact heat exchanger (isometric view).....	50
Figure 37: Cross-section view of the 3D heat exchanger model. 4 out of 11 flow channels are labeled in red.....	51
Figure 38: Heat exchanger dimensions.....	52
Figure 39: Inlet/outlet dimensions	52
Figure 40: Inlet and wall thickness dimensions	52
Figure 41: Dimensions of the flow channel grid within the heat exchanger	53
Figure 42: Mass properties of the heat exchanger model calculated through SolidWorks analysis tools if the model was made out of neat epoxy	53
Figure 43: 3D model of flow channels	54
Figure 44: Left side view	55
Figure 45: Top view	55
Figure 45: Bottom view	55
Figure 47: Flow channel dimensions	56
Figure 48: Mass properties of the flow channels model calculated through SolidWorks analysis tools if the material of the model is neat epoxy	56
Figure 49: Filaments of ABS material used in 3D printing.....	57
Figure 50: 3D printed heat exchanger model. Some parts of the model that have 90° corners and edges	58
Figure 51: 3D printed flow channels. Part of the model that experiences the largest stress due to the top opening is circled in red.....	59
Figure 52: Design and fabrication of a compact polymer heat exchanger flowchart	60
Figure 53: AeroMarine silicone product.....	61
Figure 54: Purchased beeswax	62

Figure 55: Two-part silicone mold used to manufacture expandable flow channels63

Figure 56: Cured wax flow channels64

Figure 57: Silicone mold for heat exchanger fabrication, with wax flow channels that correctly fit the mold65

Figure 58: First trial of neat epoxy heat exchanger fabrication- the wax flow channels were entirely removed and there were openings at the bottom of the heat exchanger and by the outlets at the top (marked with black arrows)67

Figure 59: Aluminum fixture used to support flow channels mold68

Figure 60: Fixture-wax mold setup.....68

Figure 61: Successful trial of a heat exchanger fabrication after implementing aluminum fixture setup69

Figure 62: Compact neat epoxy heat exchanger prior to flow channels removal.....69

Abstract

Heat exchangers are widely used in different industries as primary devices to transfer heat between fluids or gases that are at different temperatures. These devices are most commonly made out of metals, which are known for their excellent thermal conductivity. However, the lifespan of heat exchangers can be limited depending on which environment they are exposed to, because metals are susceptible to corrosion. This study provides an alternative material choice to metals and suggests a fabrication method that can be used to fabricate a high-efficiency compact heat exchanger. Commercially available materials that are thermally conductive, as well as materials fabricated in laboratory, were tested and characterized for their mechanical and thermal properties, and microstructure. Materials fabricated in laboratory used neat epoxy matrix and different thermally conductive reinforcement materials: copper, graphite flakes, and graphene nano powder. The most promising results were achieved by a 35 weight % graphite flakes/epoxy laminate, with its thermal conductivity being close to 2 W/mK. Heat exchanger fabrication method involved designing and 3D printing models of the compact heat exchanger and its flow channels, which are subsequently used to fabricate reusable silicone molds. Expandable flow channels were fabricated by casting beeswax, and later removed by melting from a gravity-casted polymer, to create the geometry of a conventional heat exchanger. The final result was a neat epoxy compact heat exchanger with successfully removed flow channels. Last chapter of this thesis discusses future work recommendations and suggestions on how to move forward in this research area.

Chapter I: Introduction

1. Topic background

Heat exchanger is a device used in heat transfer applications, where heat is exchanged between fluids and/or gasses. They are utilized in different industries for fluid or gas cooling, heating, and optimizing the operating temperatures of different devices and elements, such as air conditioning, refrigeration, nuclear and chemical plants, renewable energy, automobile, and aerospace industries [1]. There is a large number of heat exchanger types, such as tubular, shell and tube, plate, plate fin, and phase-change heat exchanger. Traditional heat exchanger used for air conditioning is shown in Figure 1 below. It is a plate and fin heat exchanger made out of copper fins and aluminum plates. Air flows between the aluminum plates and efficiently transfers heat to the device.



Figure 1: Plate and fin air conditioning heat exchanger (*image courtesy to grabcad.com*)

Since the primary purpose of heat exchangers is to effectively exchange heat between two media at different temperatures, they are almost always built out of metals, such as copper, copper-nickel, aluminum, carbon steel and stainless steel, due to their effective thermal conductivity [1]. Some of the issues that commercial heat exchangers are experiencing is their large size, weight, and metal corrosion that shortens their lifespan. Therefore, there has been a large demand for smaller heat exchangers that are much lighter, cheaper, and yet equally effective in performance. Such devices are called compact heat exchangers (CHE). Due to their much smaller size compared to the traditional heat exchanging devices, they are mostly used in industries where size reductions would offer large cost savings [2]. An example of extensive utilization of compact heat exchangers can be found in transportation and power plant industries. The rotating distillation unit HiGee reduced the size of their process plant to just a few meters in height after utilizing compact heat exchangers in their power plant. Knowing the potential and advantages that compact heat exchanger can bring in various applications, it is interesting to see that they only account for around 10% of the worldwide heat exchangers market [3]. This implies that, although already being implemented in several different industries, there is a considerable potential for improvement of these devices so that they can have a more widespread use.

2. Literature review

2.1. Polymer heat exchangers

Polymers are molecules that contain a large number of reoccurring subunits. They can be divided in the two most common groups: natural and synthetic. Natural polymers, as the name itself suggests, can be found in the nature or manufactured with natural materials, such as silk, wood, cellulose and rubber. On the contrary, synthetic polymers are made with organic materials whose combination can be altered in order to satisfy the performance requirements [3]. Using synthetic polymers in manufacturing heat exchangers is becoming a trending research topic in composite and polymer materials research; several research groups have conducted different studies in an attempt to replace the currently used metals and their alloys with a polymer that performs well and adds more advantages to the manufactured device. DuPont et al. were the first to research the

use of polymers in heat exchangers [4]. With polymers not being prone to corrosion, requiring much simpler fabrication methods, and successfully enduring exposure to both liquids and gasses, they offer a great alternative for metals in heat exchanger fabrication. The greatest advantage of using polymers that resolves the above described weight and cost issue lays in their structural flexibility which can significantly decrease the volume of the manufactured device, therefore reducing the overall weight and cost associated with it. It has been reported that producing a unit mass of polymers requires almost two times less energy needed to produce a unit mass of metals that are usually used in heat exchanger fabrication [1]. Therefore, it is evident that by substituting metals with polymers will offer many advantages for heat exchanger performance, manufacturing, and durability.

The most important criteria in choosing a material other than metals to fabricate heat exchangers is its thermal conductivity. Some of the most commonly used polymers in the industry are Teflon or PTFE (polytetrafluoroethylene), PC (polycarbonate), PVDF (polyvinylidene fluoride), and PE (polyethylene) [5]. Given that polymers have significantly lower thermal conductivity than metals used for heat exchangers [6], different additive materials that could possibly be added to the polymers to make them more suitable for the heat exchanger applications have been researched. The most commonly studied reinforcement materials/fillers are metals, carbon, and carbon-based materials [7]. Epoxy, a polymer that has a low cost and very simple fabrication method is not among the most commonly used materials for manufacturing heat exchangers most likely because of its low thermal properties (referring to pure epoxy, consisted of resin and hardener). However, epoxy-based compounds have lately been receiving more attention because they can contain various reinforcement materials, and, therefore, even further simplify the overall manufacturing process. Therefore, it is motivating to explore how to reinforce epoxy with a thermally conductive material/filler to make a more suitable polymer for heat exchanger applications. The majority of the research articles about manufacturing a high thermal conductivity composites that are using neat epoxy are discussing results after introducing carbon/graphite particles and their byproduct fillers. The laboratory experiments conducted for this thesis also include research on using copper and aluminum fillers to achieve high thermal conductivity composite material, which will be further discussed in the next chapter.

Mamunya et al. [8] investigated a hybrid polymer fabricated out of copper and nickel powders and either PVC (polyvinyl chloride) or epoxy matrix. The size of the powder particles ranged between 10 and 100 μm . They randomly distributed Cu and Ni particles in each of the trials. When dispersing Cu particles in the epoxy matrix at 30% volume ratio, the maximum obtained thermal conductivity was 1.72W/mK. This may suggest that increasing the volume percentage of Cu particles would consequently increase the composite thermal conductivity coefficient, but the experiments have proven differently. Mamunya et al. concluded that each matrix-filler combination has its unique parameter that optimizes their volume percentages to achieve the highest possible thermal conductivity. They referred to this relationship as the packing factor F , which is determined by comparing conductive phase topology and the shape of reinforcing particles. For the Cu-epoxy case, they found that $F=0.51$.

Xu et al. [9] wanted to explore if a thermally conductive polymer with epoxy matrix can be obtained if aluminum nitride (AlN) or silicon carbide (SiC) whiskers and particles were added to it. The fabrication process included mixing, degassing, and curing at a room temperature of the filler-epoxy mixture. When adding AlN fillers, much better results were achieved; the highest thermal conductivity obtained was 11.5 W/mK for a 1:25.7 ratio of whisker-to-particle volume percentage, with a total volume filler fraction of 60%.

Wang et al. [10] conducted a series of experiments by reinforcing epoxy matrix with liquid-crystalline fibers. They individually introduced Vectra, Zylon AS, and Zylon HM fibers, known for their high strengths, and observed how they interact with the epoxy matrix in terms of thermal conductivity. Their thermal conductivity results for epoxy reinforced with Zylon AS fibers ranged between 19 and 23 W/mK, which seemed to be an excellent result. Further tests of the obtained composite yielded that this structure is somewhat unstable because its thermal conductivity decreased whenever the surrounding temperature was increased. This happened most likely due to the fiber expansions and misalignments, which highlights the importance of choosing the appropriate filler for different applications. In terms of fabricating compact heat exchangers, it is evident that this kind of fibers would not be the best choice. Although the resulting thermal conductivity coefficient is high, its structural instability under high temperatures does not make it an appropriate material candidate.

As mentioned before, one of the most researched reinforcement materials for epoxy polymer composites is carbon. Carbon comes in various shapes and sizes and, when altered, comes in a form of graphite, graphene, carbide, etc. Many carbon-based compounds can be combined with polymers to achieve improved thermal and mechanical properties. Moreover, using a hybrid mixture (two or more components) is also very common when working with materials from the carbon family. Mahanta et al. [11] have done a remarkable research on this topic, which resulted in them obtaining a US Patent for the composite fabrication method in 2018 (patent number: US10125298B2). Graphite and graphene were used as reinforcement materials and combined into 7%, 14% and 35% groups according to their overall weight percentage (a total of 13 samples). The mixture was ultrasonicated and magnetically stirred in acetone for 4 hours, after which the epoxy and resin were added. The mixture was also degassed when needed to remove any trapped air and, finally, press molded and cured for 6 hours at 90°C. Table 1 shows graphite-graphene ratios for all three weight percentage groups.

Table I: Different weight and volume percentage of graphite-graphene hybrid [11]

	<i>Weight percent (%)</i>		
	Graphite	Graphene	Epoxy
Group 1 (graphite + graphene = 7wt%	0	7	93
	1	6	93
	2	5	93
	3	4	93
	4	3	93
	5	2	93
	6	1	93
	7	0	93
Group 2 (graphite + graphene = 14wt%	10	4	86
	12	2	86
	14	0	86
Group 3 (graphite + graphene = 35wt%	30	5	65
	33	2	65
	35	0	65

It was observed that filler weight percentage higher than 35% caused difficulties in stirring the mixture, which is why 35% is chosen as the optimum filler-to-epoxy ratio. The highest thermal conductivity of 42.4 W/mK among 13 samples was found in Group 3, with 30:5 graphite-graphene weight percentage ratio.

On the other hand, Chen and Ting [12] were able to achieve thermal conductivity over 15 times higher compared to what Mahanta et al. [11] were able to obtain, by using vapor grown carbon fiber (VGCF) as their epoxy matrix reinforcement material. The VGCF mats were grown by using a substrate-growth technique (fibers are grown on a film (substrate) of the same material, resulting in a higher purity compared to the material film), while being treated to a temperature over 2500°C. The mats were then placed in a mold after which the epoxy was poured over. The mold was then placed under 1000 psi hot press at 150°C for 15 minutes, after which it was left to cure at the room temperature. This fabrication process yielded a thermal conductivity of 695 W/mK with a density of 1.5 g/cc. These impressive results would most likely require very sophisticated equipment to be replicated, but this study goes on to prove the versatility and advantages of reinforcing epoxy polymer with carbon fillers.

2.2. Improving thermal conductivity in polymer heat exchangers

Now that it is evident that it is possible to reinforce a polymer, such as epoxy, with thermally conductive materials, the next step in this topic is to determine different ways to further improve this characteristic. Several different approaches have been documented, with one of them being that a hybrid filler should be used instead of a single filler. As mentioned in Mahanta et al. [11], they used graphite flakes and graphene nano powder as their fillers, since graphene would provide additional connection between the graphite flakes, therefore improving and reinforcing the filler network, which eventually resulted in very high thermal conductivity values.

Bard et al. [7] have researched whether thermal and electrical conductivity of carbon fibers will be improved if they were coated with either nickel or copper. The fiber volume content of their laminates was around 50%, and the thermal conductivity of the laminate with uncoated fibers was 3 W/mK. After introducing the nickel coating, this value went from 3 to 6 W/mK.

Furthermore, their copper coating yielded even better results; the thermal conductivity of the laminate was around 20 W/mK. However, these values were measured in the fiber direction, whereas the thermal conductivity values obtained in the through-plane direction were around 10 times smaller. The initial thermal conductivity of the laminate in a direction transverse to carbon fibers was 0.6 W/mK. After coating the fibers with nickel and copper, the thermal conductivity values increased to 0.9 and 2.9 W/mK, respectively. This research has proven that adding different elements to a composite material, such as carbon-epoxy, will noticeably enhance its thermal conductivity, but only in certain direction. Thermal conductivity in the through-plane direction is more significant for the heat exchanger application in the through-plane direction. Nevertheless, an improvement in thermal conductivity by coating carbon fibers with another element has been shown in both through-plane and along-fiber directions, which indicates that the thermal conductivity of a polymer composite used for heat exchanger fabrication can also be improved.

In the work of Xu et al. [9], the highest thermal conductivity results were reported when the material fillers were a whisker-particle combination of aluminum nitride (AlN). However, one of the attempts was to use only AlN particles and determine their effect on the thermal conductivity improvement. The highest values were obtained when the largest AlN particle size was used (115 μm), but the implication of using particles of such size was that there was a large number of porosities within the composite, resulting in a bad quality laminate with low thermal conductivity. To alleviate this effect, the AlN particles underwent a silane surface treatment, which decreased the thermal contact resistance between the particles and the epoxy matrix, which, in return, decreased the porosity level within the laminate. The thermal conductivity reported after introducing this surface treatment to the fabrication process was 11.0 W/mK, slightly lower than when the AlN whisker and particles combined were used. The advantage of this process is that only a single form of AlN was used instead of two, which contributes to the lower manufacturing cost. Hence, this study shows that a simple addition to the fabrication process, such as a silane surface treatment, can be effective in improving both the structural and thermal conductivity of a laminate.

Similarly, Cui et al. [13] explored if coating multi-walled carbon nanotubes (MWCNT) with silica (SiO_2) will enhance the thermal conductivity of the epoxy matrix composite compared to

the uncoated MWCNT [13]. The motivating claim was that, through a synthesis by a sol-gel method, coating MWCNT with silica will improve their connection and bonds. Their results show that thermal conductivity of the composite increased by 51% when they used 0.5 weight % of the fillers, and 67% when they used 1 weight %. Furthermore, the addition of silica increases electrical resistivity of the laminate, which can bring advantages in heat exchanger fabrication.

Carbon nanotubes are one of the most sophisticated byproducts of the carbon family that display great mechanical properties. When used as a filler in a polymer composite material, the dispersion and arrangement of the fibers is somewhat hard to control because this kind of fibers tends to cluster and form irregular agglomerations. The nonhomogeneous areas formed by these clusters greatly affects the laminate quality. The work by Fan et al. [14] has shown that when a dispersion of fillers within a laminate improves and becomes more uniform, the filler network itself becomes much stronger, meaning that the laminate quality is also improved.

Yue et al. [15] have researched whether the dispersion issue of carbon nanotubes can be solved by introducing another filler from the carbon family-graphene nanoplatelets. Both CNT (carbon nanotubes) and GNP (graphene nanoplatelets) in different ratios (8:2, 6:4, 4:6, and 2:8, respectively) were magnetically stirred and sonicated prior to being added to the resin. The mixture was degassed to avoid any unwanted trapped air and, after cooling down at the room temperature, mixed with a hardener and cured also at the room temperature (which was followed by a post cure for 15h at 60°C). The results show that the flexural properties of the laminate have been increased, especially for the CNT:GNP ratio of 8:2, which implies that the filler network within the laminate has been improved [14]. Furthermore, improvement in the filler network also means that the dispersion of the fillers has been enhanced, resulting in a laminate with a much more uniform structure. This uniformity indicates a better connection between the CNT and GNP particles throughout the laminate, which will result in its improved thermal conductivity as well. Once again, this study shows the benefits of introducing additional fillers to a composite material to enhance its filler network. For the heat exchanger applications, conducting a similar method in improving the thermal conductivity of a composite polymer would most likely result in the increase of its value.

Another approach in improving the thermal conductivity, besides using hybrid composite materials, is adjusting the fabrication process through different methods. Li et al. [16] explored how in-situ exfoliation of graphite nanoplatelets (GNP) through three-roll milling (TRM) can improve quality of the graphite dispersion. Their GNP were mixed with epoxy and passed 8 times through the three-roll milling machine at 200 rpm. The last six passing had a force of 5N/mm constantly applied through the mill and the milling temperature ranged between 24 to 40°C. Once the milling was completed, the mixture was combined with a hardener, degassed, and cured at the room temperature for 24 hours. Final results confirmed through several imaging techniques, such as scanning electron microscopy (SEM), X-ray diffraction (XRD) and Raman spectroscopy indicated that the graphite nanoplatelets were well distributed and uniformly connected throughout the laminate. Along with the findings from Yue et al. [15], it is evident that because of the structural improvement of the composite laminate, a further processing of the GNP-epoxy mixture with three-roll milling will result in a good-quality polymer, which consequently has a great potential to improve its thermal conductivity as well.

3. Topic scope and proposed research

This research aims to enhance the performance of compact heat exchangers by altering the fabrication method and substituting the material used in such process; replacing metals with thermally conductive polymers. The end result will be a compact heat exchanger fabricated with a high thermal conductivity polymer. The two main parts of this research will be: (i) developing a new polymer composite with an epoxy matrix and thermally conductive reinforcement material(s), and (ii) a design and fabrication method for such heat exchanger. By conducting this research and implementing our findings, what we aim to achieve, compared to the commercially available compact heat exchanger, is:

Reduction in weight: The metals that are currently used in heat exchanger fabrication can add a lot of weight to the final product. For compact heat exchangers especially, this can impose a significant issue in different applications. Our goal is to achieve the weight reduction by making a polymer composite with epoxy matrix containing micro or nanoscale fillers. It is important to find the appropriate balance between how well a filler may conduct heat and how much of it is

needed. In theory, the more thermally conductive filler is used, the better the heat transfer properties will be achieved. Metal fillers will most likely be great heat conductors, but the weight of the heat exchanger may be compromised if it is discovered that large amounts are needed for good thermal conductivity performance. Therefore, a successful weight reduction without compromising thermal conductivity of the material can only be achieved by using fillers that have low densities so that the overall heat exchanger weight is reduced, and yet the thermal conductivity performance stays the same.

Reduction in cost: The cost of materials that are used to fabricate the polymer heat exchanger will be significantly lower than the cost of fabricating a metal heat exchanger. The largest cost associated with this production comes from the thermally conductive fillers. Our aim is to find a relatively inexpensive filler with excellent thermo-mechanical performance. This will be achieved by either using smaller amounts of expensive fillers or finding a relatively inexpensive filler that performs just as well at higher filler loading.

High thermal conductivity: For compact heat exchangers and its applications, we aim to achieve a thermal conductivity of 3 W/mK or higher. We will compare several material candidates and their thermal conductivity performance and determine which one(s) can potentially deliver the expected results. As mentioned previously, it is important to find a good filler-to-matrix ratio so that the weight of the heat exchanger is not significantly increased.

High durability: Corrosion is a well-known issue that metals experience over time, hence limiting the performance and lifetime use of a product, including heat exchangers. We will increase the compact heat exchanger's durability by replacing metals, since polymers are materials that are not susceptible to corrosion.

Waste reduction and recyclable materials: Metal processing can yield a lot of waste material that cannot always be recyclable. Our goal is to minimize the waste production and offer alternative fabrication methods that will contain recyclable and non-toxic materials.

Chapter II: High Thermal Conductivity Composite Materials

1. Objective

This chapter describes the analysis of candidate polymer materials and their composites that are suitable for the compact heat exchanger application. First part consists of characterizing commercially available materials whose properties would be suitable for this project, whereas the second part consists of finding the most suitable matrix and reinforcement additives that can be manufactured into a laminate and, eventually, a compact heat exchanger. Density, mechanical, thermal and microstructure morphological properties of the candidate materials were determined through TGA, DMA, laser flash, SEM and three-point bending flexural tests, and the results were used to perform a comparative analysis to determine a suitable material choice.

2. Materials

2.1 Commercially available materials

Finding a suitable material candidate that is commercially available would be useful to expedite the development of high-efficiency heat exchangers. It was concluded that the best materials would be the ones with an epoxy matrix and metal reinforcement particles/fibers. This is due to the fact that epoxy is a very versatile polymer in terms of fabrication and mixing with different materials, and because metals are the best heat conductors. Therefore, a set of important properties for such materials was determined in order to choose appropriate material candidates:

1. Thermal conductivity- One of the most important characteristics of the chosen material is thermal conductivity. The reinforcement material in this product must be thermally conductive in order to be suitable for compact heat exchanger applications. The overall thermal conductivity of the cured laminate is preferred to be 2 W/mK or higher.
2. Electrical conductivity- The material should only be thermally conductive; there should be little to no electrical conductivity in order to avoid interference between compact heat exchanger and other installed devices. This is a secondary concern and may

not disqualify a material if its thermal conductivity and mechanical properties are satisfactory.

3. Useful temperature range- Since compact heat exchangers may be used in high temperature environments, a wide temperature range is preferred. A service temperature up to 60°C or 70°C would be suitable for several industrial applications.

4. Price- The goal is to find affordable yet effective material candidates that can substitute the use of metals in heat exchangers. Therefore, the overall price of the material should be reasonable and justified by the material properties.

The first selected material was from the Freeman Manufacturing and Supply company that carries numerous types of metal-reinforced epoxies. The most commonly used reinforcement materials in their products are iron, silver, and aluminum. Table 2 shows the selected Freeman products that were further analyzed for their properties.

Table 2: Freeman products that may be suitable for heat exchanger applications

Product Name	Mix Ratio (by wt.)	Mix Ratio (by vol.)	Gel Time @72F	Demold (hours @72F)	Viscosity (cps)	Compressive Strength (psi)	Tensile Strength (psi)	Reinforcement Material
Freeman 801	100:12:00	100:23:00	150	24	4,650	12,500	7,280	Aluminum
RenCast 3269	100:09:00	100:18:00	140	24	4,300	14,400	8,700	Aluminum
RenCast 3215-2	100:18:00	100:35:00	200	24	3,600	11,100	4,900	Iron
RenCast 3215-3 mix 1	100:30:00	100:57:00	70	24	6,200	12,600	4,300	Iron
RenCast 3215-3 mix 2	100:40:00	100:76	65	24	5,400	Soft	1,200	Iron
RenCast 3215-3 mix 3	100:50:00	100:95	60	24	4,600	Rubbery	300	Iron
RenCast 3253	100:05:00	100:16:00	100	24	7,500	15,200	7,100	Iron

Out of several chosen and discussed options, the following Freeman products were selected, summarized in Table 3 below:

Table 3: Selected material candidate from Freeman products for heat exchanger applications

Type	Name	Quantity	Unit Cost
Epoxy	Freeman 801 Epoxy Resin	1 quart	\$29.04/q
Hardener	Freeman 801 Epoxy Casting Hardener	1 pint	\$14.72/p

The reason behind choosing this Freeman set of products over others listed in Table 1 is because of its favorable gel time, viscosity, and both compressive and tensile strengths. Moreover, the fact that this product was readily available for purchase was also influential to choose this product. However, the only downside of this material is that its heat conductivity coefficient is not known; it is only known that the used reinforcement material is aluminum. Freeman company did not have the information regarding the thermal conductivity values, but a series of tests can be conducted in the future to determine the thermal properties of Freeman 801 epoxy.

Epoxies company also carries a variety of metal-reinforced polymer products. In terms of cost, it was significantly less expensive than the chosen Freeman product. Table 4 shows the summary of information regarding the Epoxies products selected for further investigations.

Table 4: Selected material candidate from Epoxies products for heat exchanger applications

Type	Name	Quantity	Unit Cost
Epoxy	70-3812 NC High Thermal Transfer Epoxy	1 quart	\$51.00/q
Hardener	70-3812C Hardener:1	1 quart	\$52.84/q

This set of products was chosen because its properties are very similar to that of the purchased Freeman product. However, a significant difference between these two products can be found in its viscosity value, shown in Table 5 below. The viscosity of the Epoxies resin is almost the double of the Freeman's epoxy viscosity. Furthermore, curing schedule time is 7 times less for

the Epoxies resin. Therefore, it was concluded that it would be beneficial to compare these two products. Comparison of other properties of both products are presented in the table below. Thermal conductivity of the Epoxies product was given as 4.5 W/mK.

Table 5: Freeman vs. Epoxies product properties based on the data from the supplier

Product	Particle Type	Mixed Viscosity (cps)	Mix ratio by wt. %	Tensile strength (MPa)	Specific gravity of mixed resin	Thermal conductivity (W/mK)	Curing schedule (room temp.)
Freeman	Al	4650	100:12	50.2	1.70	-	7 days
Epoxies	Al	8000	100:10	55.2	1.81	4.5	24 hours

2.2 Composite materials prepared in the laboratory

Another aspect of finding a thermally conductive material appropriate for compact heat exchanger applications was to determine if such materials can be prepared in laboratory. Commercially available epoxy is chosen as a suitable matrix material throughout this process. The selected epoxy type was EPIKOTE™ Resin MGS™ RIMR 135 and EPIKURE™ Curing Agent MGS™ RIMH 137, both supplied by EPIKOTE™. The cure cycle is 24h at room temperature followed by a post cure of 15h at 80 °C. Additional properties of this epoxy as provided in the supplier’s datasheet are shown in Table 6.

Table 6: EPIKOTE™ product properties from supplier’s datasheet

EPIKOTE™ Epoxy properties from the material data	
Density [g/cm³]	1.18 – 1.20
Flexural strength [N/mm²]	90 – 120
Modulus of elasticity [kN/mm²]	2.7 – 3.2
Tensile strength [N/mm²]	60 - 75
Compressive strength [N/mm²]	80 - 90
Elongation of break [%]	8-16
Impact strength [KJ/m²]	70 - 80

Using the same matrix material allows for a better comparison of performances of different reinforcement materials. The selection criteria in choosing the appropriate fillers are as follows:

1. The filler particles should be of a spherical shape or flakes.
2. The size of the particles is preferred to be indicated in technical data sheets provided by the vendor carrying the product. Smaller sizes are expected to perform better and yield more homogeneous properties.
3. The powder purity is preferred to be higher than 93%. The higher the purity values are desirable, as long as the cost is not excessive that would prevent the material to be adopted at an industrial scale.

The selection of the filler material was narrowed down to three metals: aluminum, iron, and copper. Al, Fe, and Cu were chosen because these metals are the most accessible products on the market. Average aluminum thermal conductivity coefficient is, $k = 236 \text{ W/mK}$ and it increases with the increase in temperature. Iron, on the other hand, has approximately $k = 69.4 \text{ W/mK}$, and this value is decreasing as the surrounding temperature increases. Copper is the metal which has the highest thermal conductivity coefficient out of these three materials, $k = 392 \text{ W/mK}$. Given the difference in k values, it was concluded that the copper powder should be selected. Moreover, copper is well known for its great thermal conductivity and is expected to serve well as a reinforcement material. Table 7 shows the summary of the copper powder properties, sold by Sigma-Aldrich, Co (326453). and Figure 2 shows its SEM image.

Table 7: Sigma-Aldrich, Co. copper powder

Material	Form	Particle size	Density (g/mL)	Purity	Cost
Cu	Powder (spheroidal)	10-25 micrometers	8.94	98%	\$135/kg

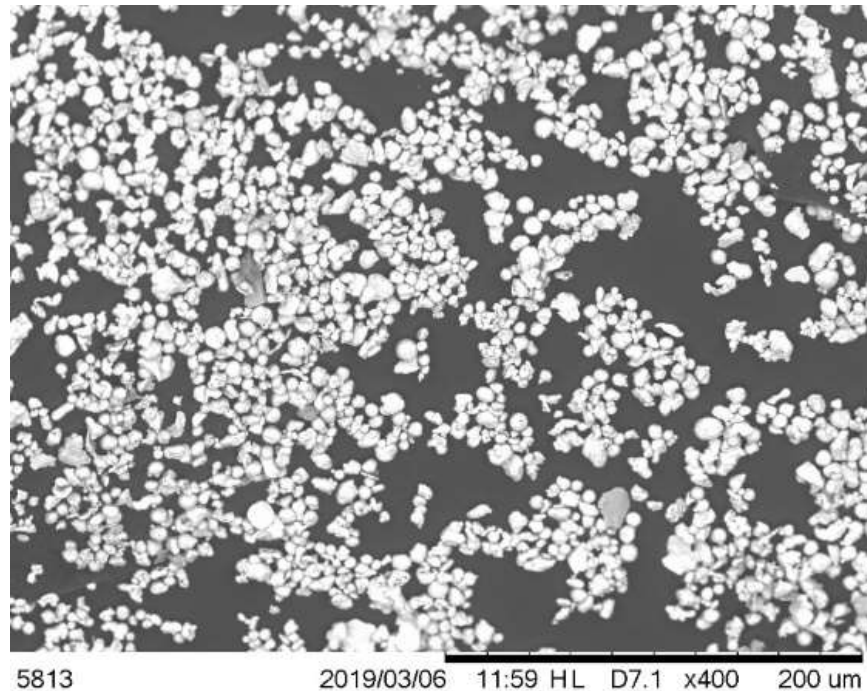


Figure 2: SEM image of the copper powder as received (Sigma-Aldrich, Co.)

Another reinforcement material candidate was graphite. Based on previous research, it was evident that desired thermal conductivity could be achieved when using graphite. The work presented by Mahanta et al. [11] shows that by using two graphite byproducts, graphite flakes and graphene nano powder, the highest achieved thermal conductivity value was above 30 W/mK. Therefore, replicating the same fabrication process presented by Mahanta et al. was attempted in this investigation. The first part of this process was to identify whether a single product (either graphite flakes or graphene nano powder) can be independently used to achieve the desired thermal conductivity. Graphite flakes were purchased from Asbury Carbons, Co. (item #3807 SEFG) at a cost of \$83.24 for 5lb of product (98.9% purity). The average surface area of these flakes is 17.3 m²/gram. Figure 3 shows the SEM image of the flakes.

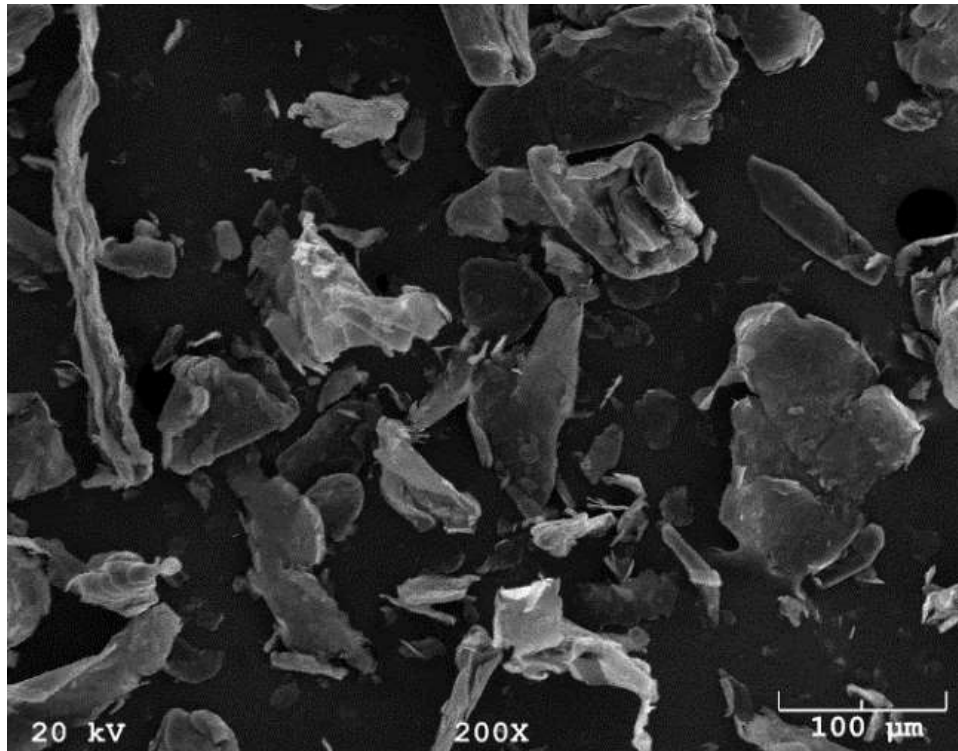


Figure 3: SEM image of Asbury Carbons graphite flakes

Mahanta et al. [11] were able to achieve exceptional thermal conductivity value by combining graphite flakes with graphene nano powder (GNP). Their reasoning behind using two components was that the addition of nano powder would enhance the filler network by serving as a connecting medium between the graphite flakes, while being thermally conductive itself. The graphene nano powder was purchased from Asbury Carbons, Co. (item Nano3017) for \$53.90 per 1lb. Average surface area of the particles is $350 \text{ m}^2/\text{g}$, true density is 2.16 g/cc and the carbon percentage (purity) is 99.94%. SEM image of this product is shown in Figure 4 below.

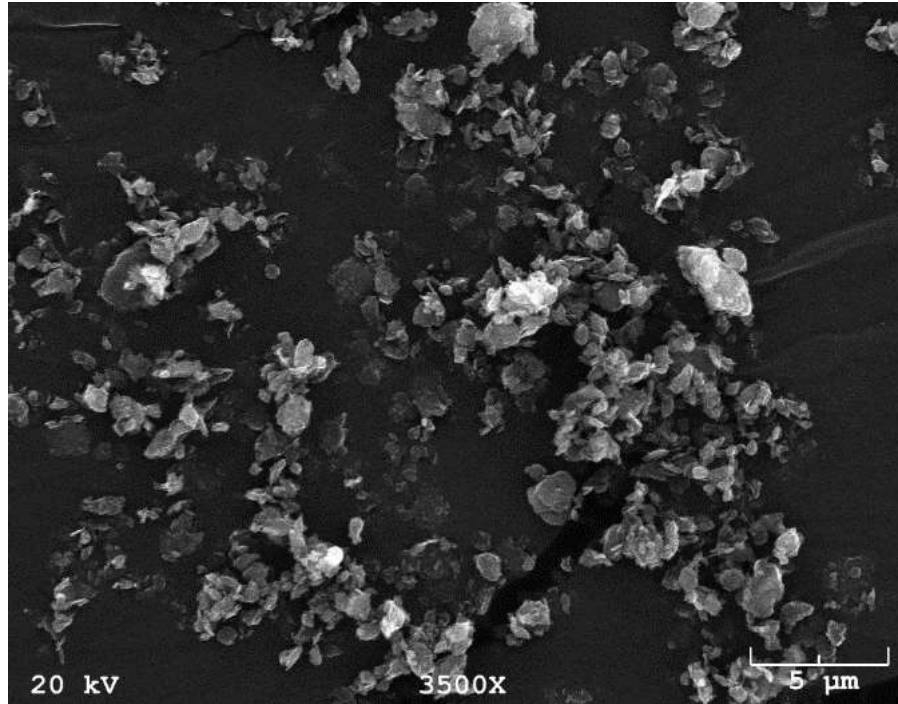


Figure 4: SEM image of Asbury Carbons graphene nano powder

3. Fabrication methods

Both Freeman and Epoxies laminates were fabricated by gravity casting. 79.38 grams of Freeman resin was mixed at 350 rpm for 5 minutes, at room temperature. The uniform mixture was poured in a silicon mold (150mm x 150mm x 1mm) and, according to the supplier instructions, cured at the room temperature for 7 days. 96.08 g of Epoxies resin was used to fabricate the laminate. It was mixed at 350 rpm for 5 minutes and cured at room temperature for 24 hours in a silicone mold with the same dimensions. Figures 5 and 6 show cured Freeman and Epoxies laminates, respectively. Images were taken with an optical laboratory microscope.

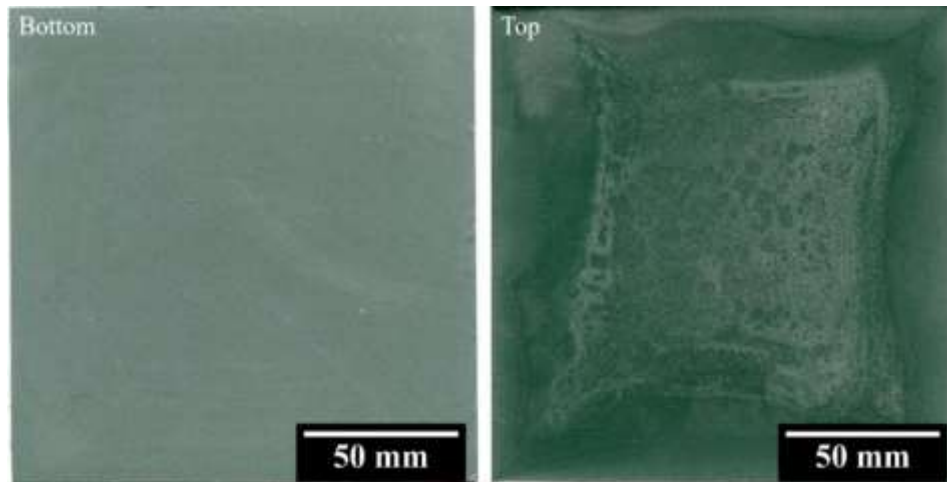


Figure 5: Freeman laminate (bottom and top)

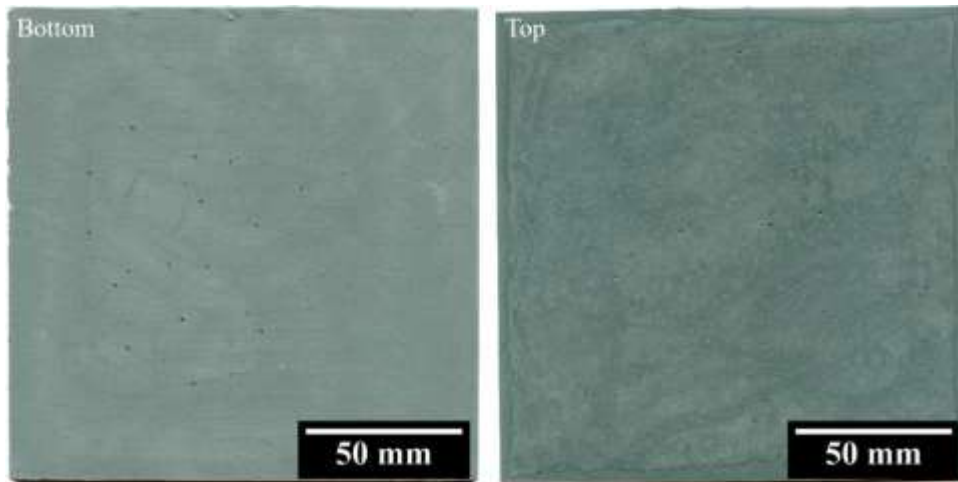


Figure 6: Epoxies laminate (bottom and top)

Neat epoxy laminates were also fabricated through gravity casting, by mixing resin to hardener in a 3:1 ratio, followed by mechanical stirring at 350rpm for 15 minutes. Different copper weight percentages were fabricated with a similar procedure (20, 300, 500 and 600 copper weight %). 20% Cu laminate was fabricated by mechanically mixing 59.96 grams of resin and copper, and it was gravity casted and cured at a room temperature in a 150mm x 150mm x 1mm silicon mold. 300% Cu was fabricated by using a total amount of 208.34 grams of copper and resin. The larger the Cu weight percentage, the harder it was to obtain a uniform copper-epoxy mixture, Figures 7 and 8 shows the microscopy image of the 20% Cu and 600% Cu laminates, respectively.

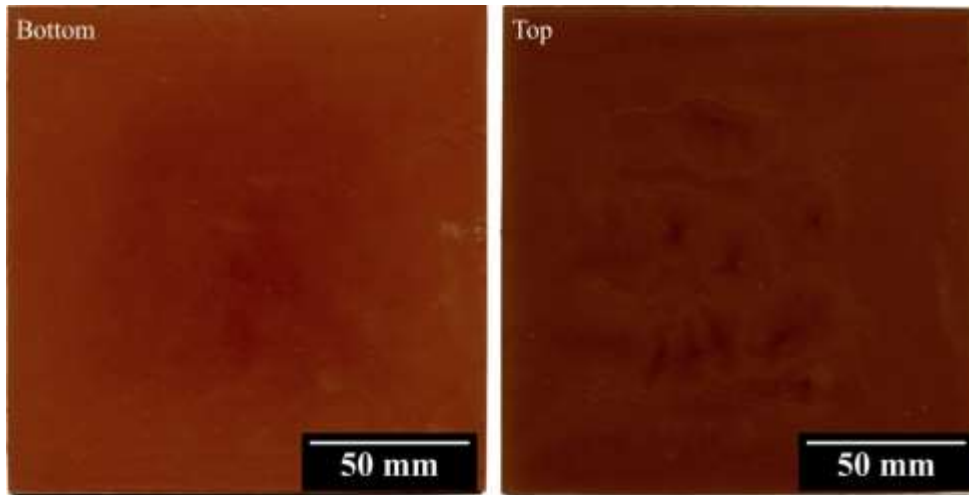


Figure 7: 20% Cu/ EPIKOTE™ RIMR 135+RIMH 137 laminate (bottom and top)

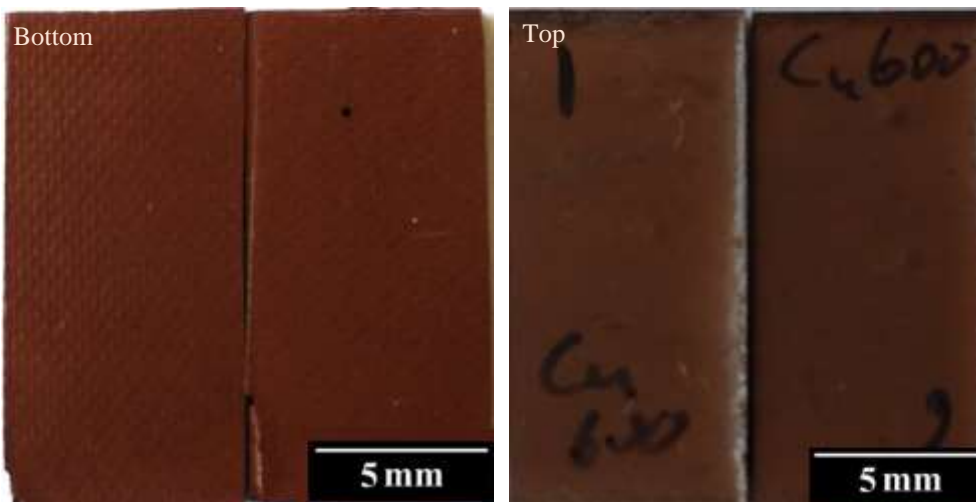


Figure 8: 600% Cu/ EPIKOTE™ RIMR 135+RIMH 137 laminate (bottom and top)

The main goals in fabricating a graphite-epoxy laminate was to achieve very little to no variation in thickness, smooth surface and uniform distribution of graphite flakes throughout the laminate. Laminates with four different graphite weight percentages were fabricated: 7, 14, 20 and 35 weight percent. The sample preparation process was as follows:

(i) Appropriate graphite weight percentage was added to the epoxy resin. The mixture was infused with acetone (~5% of the graphite + resin + hardener weight) in order to allow for a more uniform mixing of the two components. Then, it was magnetically stirred for 1 hour at 70 °C. The mixture was then placed in a vacuum oven for 3 hours at 40 °C to remove any remaining

acetone. Once the acetone was entirely removed, hardener was added to the mixture (1/3 of the epoxy weight) and mechanically stirred for 15 minutes.

Developing a curing process for this laminate was a somewhat challenging task, as it was observed that the laminate may require post cure after the initial room temperature cure and gravity casting. All laminates were casted in a 150mm x 150mm x 1mm silicon mold. When large weight percentages of graphite were added (20 and 35%), the viscosity of the mixture was too high, which resulted in agglomerations of the graphite flakes. Furthermore, it was difficult to perform gravity casting since the viscosity was paste-like and did not flow freely in the mold.

After curing at the room temperature, the surface roughness was high and there were lots of voids throughout the laminate. Therefore, the first attempt in resolving this issue was to gravity cast the mixture at different elevated temperatures and post-cure: (ii) 24h at 45 °C oven cure (Figure 9), (iii) 24h room temperature cure and 12h at 45 °C oven post-cure, (iv) 24h room temperature cure and 6h at 90 °C oven post-cure, (v) 6h at 90 °C oven cure, (vi) oven preheat at 40 °C and 24h room temperature cure.

These methods were somewhat helpful in reducing the surface roughness and decreasing the mixture viscosity, but the overall quality of



Figure 9: Fisher Scientific Thermo oven

the laminate was still not as expected. Lower graphite flakes weight percentage laminates as well as 20% were well fabricated with methods (ii) and (vi), but the process had to be further optimized to achieve good quality for 35% graphite laminates. The final curing procedure that yielded uniform laminate thickness with smooth top and bottom surfaces was (vii) 24h oven cure at 90 °C, pressed between two aluminum plates coated with Teflon® sheets. The resulting laminate with the 35% graphite fabricated with this method is shown in Figure 10.



Figure 10: 35% graphite/ RIMR 135 + RIMH 137 laminate fabricated using methods (i) and (vii)

As discussed previously, the first step in this project is to determine whether graphite flakes and GNP can be used independently of each other, in an attempt to reduce the overall cost of the product. Using only GNP as a reinforcement material was not considered since its small surface area would require large amounts of product to be used. Instead, it was investigated how GNP performs in conjunction with graphite flakes and whether high thermal conductivity values similar to Mahanta et al. [11] findings can be achieved with this hybrid material.

The same sample preparation method, referred to as (i), was used in this step, with both graphite flakes and GNP being added at the same time. Three different weight percentages were fabricated: 30% graphite flakes + 5% GNP, 20% graphite flakes + 15% GNP, and 15% graphite flakes + 5% GNP. The smallest overall filler weight percentage was 20% under the assumption that the higher the percentage, the better the filler network and laminate quality is (if dispersed properly). The highest overall weight percentage was 35%, in accordance to Mahanta et al. [11] setup, since it yielded the highest thermal conductivity value.

4. Characterization methods

4.1 Density, thermal, and mechanical properties

Thermal stability of each sample was measured through thermogravimetric (TGA) analysis with TA Q50 device. Thermogravimetric analysis determines the thermal stability of a material in which the mass of a small material sample is measured over time as the temperature of the sample is increased at a controlled rate. Results provide indicators on how a material/product is performing over time under elevated temperature. The sample size used for this test around 40-60 milligrams.

Elastic behaviors and glass transition temperatures were identified through Dynamic Mechanical Analysis (DMA) test with TA Q80 device. Dynamic Mechanical Analysis is a test used to characterize materials based on their viscoelastic performance under different temperature conditions. Result of this test indicates the glass transition temperature of the material which is used to identify different phase transitions. Size of the samples used in testing laminates was 2in x 0.5in for all the laminates.

Density of the laminates was determined by applying the rule of mixtures. Density of the individual laminate components was determined from the material data provided by the supplier. Thermal conductivity was measured by the laser flash analysis (LFA) by determining laminate's thermal diffusivity first, with Netzch LFA 457 MicroFlash device. Once the thermal diffusivity of the sample was determined, it was divided by material's specific heat capacity and density to obtain thermal conductivity values. The sample size diameter was 15mm, 2 heat impulse shots per sample were used which resulted in two successive diffusivity measurements, and the duration of each shot was approximately 1 second.

Mechanical properties of the laminates were determined by the three-point bending flexural test. 4 samples of each laminate were tested on Com-Ten 705SN device, the support span of the sample was determined by multiplying sample's thickness by 32.2. The collected data was processed to obtain material's strength, stiffness, and strain to failure ratio.

4.2 Microstructure morphology

Microstructure morphology of laminates was evaluated by using Zeiss NEON Field-Emission Scanning Electron Microscope (SEM) / Focused Ion Beam (FIB). SEM produces images of the material surface with a focused electron beam. Resulting images show the material composition and network structures within the material. Sample size used for all laminates was 1in x 0.75in, accelerating voltage was 3-5 kV and the magnification ranged from x50 to x30,000

5. Characterization results for the materials

5.1 Thermal properties measurements

TGA test for the Freeman laminate was performed at a heating rate of 10 °C per minute. The main expectation from the TGA test was to have a better understanding of the weight loss of the sample under elevated temperature conditions. As it can be seen from the Figure 11, the weight loss slowly started developing at approximately 250 °C. Then, there was a drastic increase in the weight loss amount at approximately 380 °C. The process started stabilizing at 540 °C. Finally, the weight loss stopped at 720 °C. The resulting particle weight/volume fraction was 38/21%. TGA verified that this material would not thermally degrade for the expected temperature range of heat exchangers

The main goal of conducting the DMA testing on this laminate was to find glass transition temperatures under different conditions. As seen in Figure 12, this laminate experiences a phase change from a solid to a rubbery state at 48.53 °C. At that temperature, its storage modulus is decreased from 680 to approximately 500 MPa. Loss modulus experiences its highest value at 55.91 °C, and then starts to decrease significantly. Tan delta represents the ratio of these two evaluation criteria, at which the glass transition happens at 72.25 °C. The reduction of storage modulus at around 48 C indicates that at temperatures above 48 °C, this material rapidly starts losing its modulus. Therefore, without modification, it may not be suitable for heat exchanger applications that require continuous operation at 48 °C or higher. Findings are summarized in Table 8.

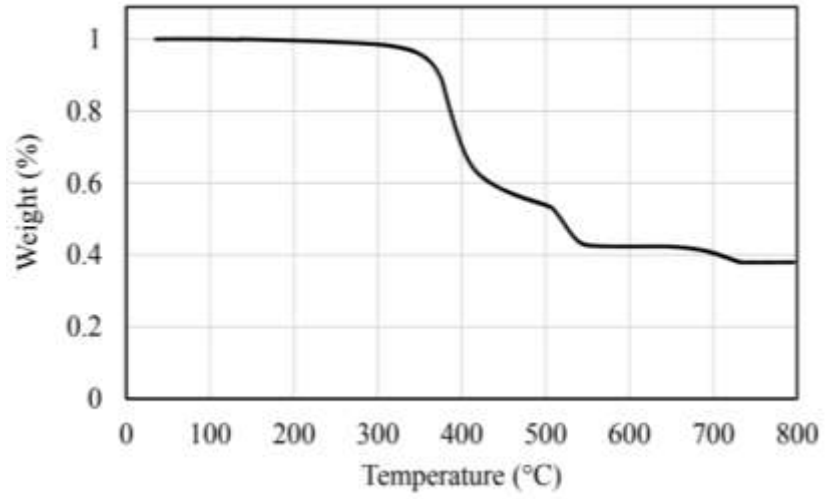


Figure 11: Freeman laminate (TGA test)

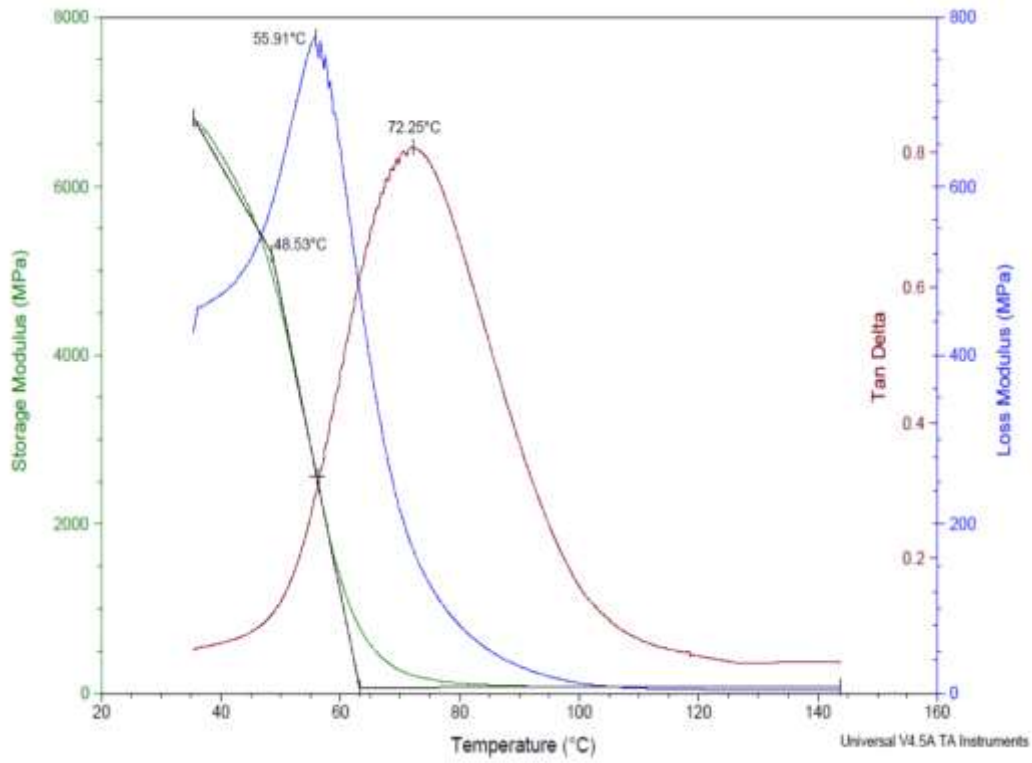


Figure 12: Freeman laminate (DMA test)

Table 8: Summary of Freeman laminate testing results

Freeman laminate- testing results	
Laminate weight [g]	79.38
Laminate density [g/cm ³]	1.495 ± 0.014
Tg by storage modulus [°C]	48.53
Tg by loss modulus [°C]	55.91
Tg by tan delta [°C]	72.25
Particle weight/volume fraction [%]	38/21

Figures 13 and 14 below shows the results of a TGA test performed at a heating rate of 10 °C per minute and the DMA test results for the Epoxies laminate, respectively. As it can be seen on Figure 13, the weight loss started and ended at approximately the same temperature values as the Freeman epoxy did. However, significantly more weight was lost during the process, which resulted in a particle weight/volume fraction of 59/37.4%. Results of the DMA test indicate somewhat lower glass transition temperature values compared to those of the Freeman laminate. According to the strength modulus (MPa), loss modulus (MPa) and tan delta ratio, the glass transition temperatures are 45.47, 50.15 and 62.23 °C, respectively. Findings are summarized in Table 9.

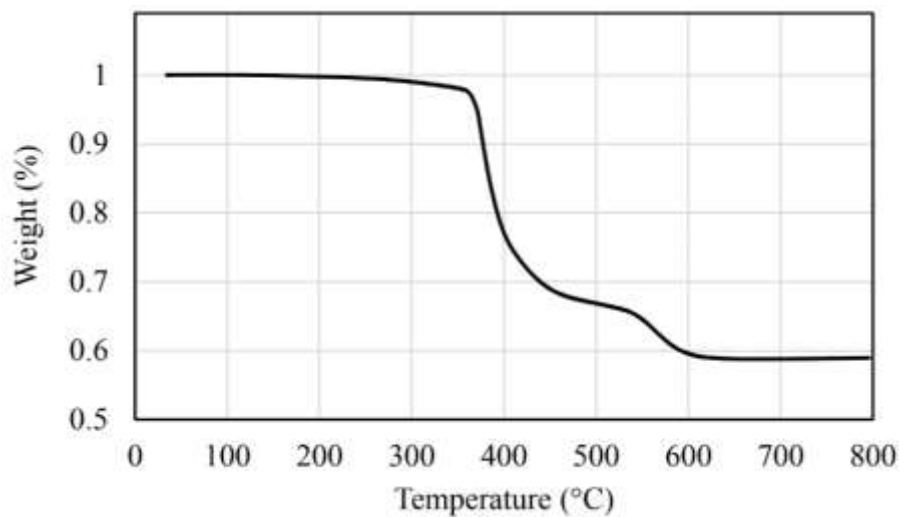


Figure 13: Epoxies laminate (TGA test)

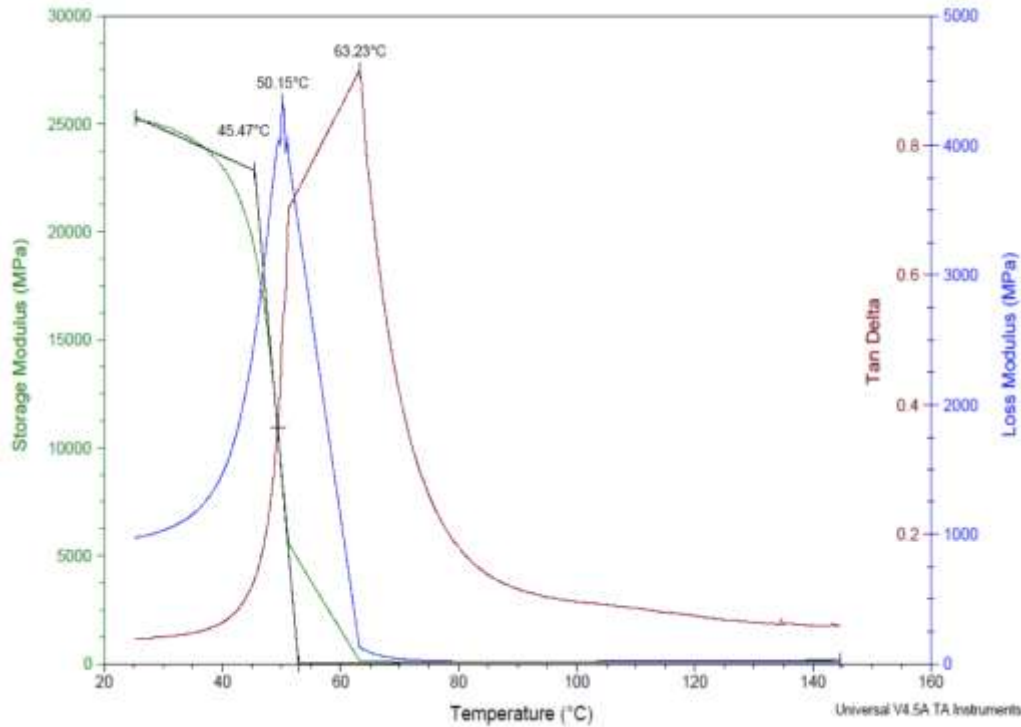


Figure 14: Epoxies laminate (DMA test)

Table 9: Summary of Epoxies laminate testing results

Epoxies laminate- testing results	
Laminate weight [g]	95.89
Laminate density [g/cm³]	1.710 ± 0.015
Tg by storage modulus [°C]	45.47
Tg by loss modulus [°C]	50.15
Tg by tan delta [°C]	63.23
Particle weight/volume fraction [%]	59/37.4

TGA and DMA test for a 120mm x 120mm x 2mm neat epoxy EPIKOTE™ RIMR 135+RIMH 137 laminate are shown in Figures 15 and 16, respectively. The glass transition temperature was found to be 90.34 °C. Other findings from both experiments are summarized in Table 10. The

results indicate that EPIKOTE™ has better thermal stability and may be used for heat transfer applications since it has a higher glass transition temperature than the other two commercial materials.

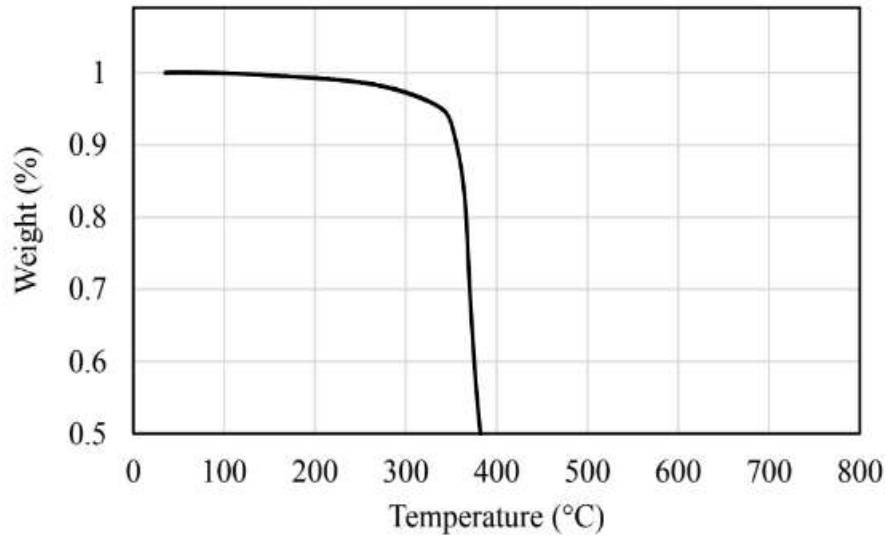


Figure 15: Neat epoxy EPIKOTE™ RIMR 135+RIMH 137 laminate (TGA test)

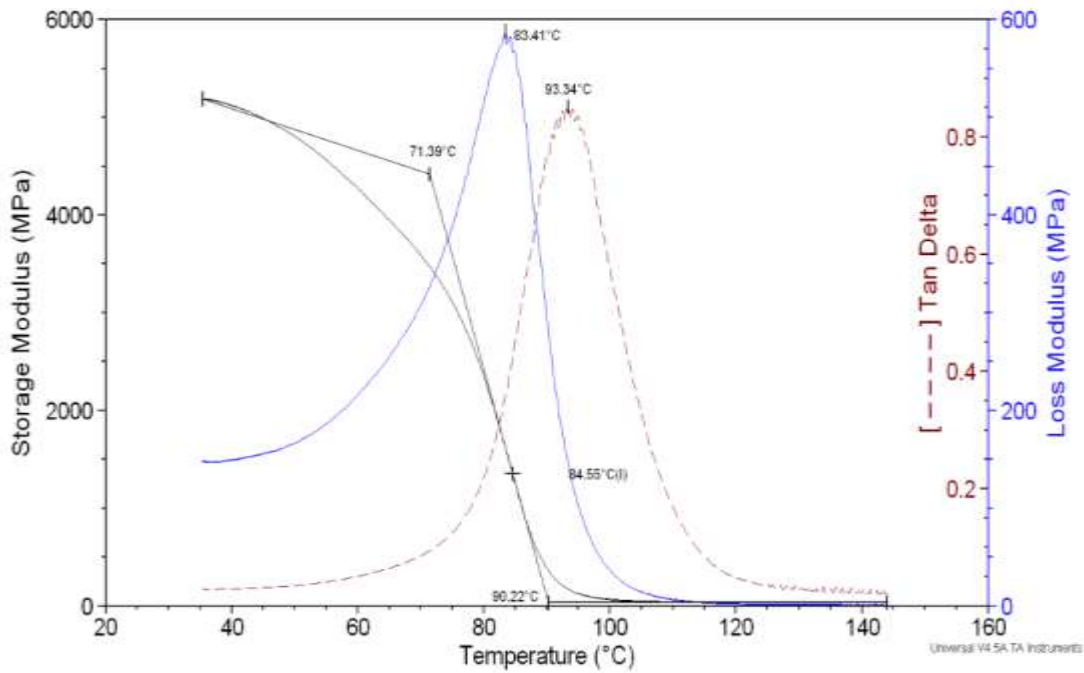


Figure 16: Neat epoxy EPIKOTE™ RIMR 135+RIMH 137 laminate (DMA test)

Table 10: Summary of neat epoxy EPIKOTE™ RIMR 135+RIMH 137 laminate testing results

EPIKOTE™ RIMR 135+RIMH 137 laminate- testing results	
Laminate weight [g]	93.2
Laminate density [g/cm ³]	1.153 ± 0.013
Tg by storage modulus [°C]	71.39
Tg by loss modulus [°C]	83.41
Tg by tan delta [°C]	93.34
Particle weight/volume fraction [%]	N/A

For a better understanding on how different copper content affects the laminate’s characteristics, different Cu weight percentage laminates will be analyzed in a comparison. Figures 17 and 18 show the TGA and DMA test results for 20% Cu laminate, respectively. Weight loss process started at approximately 330 °C and stabilized at 580 °C. DMA tests indicate that the temperatures for storage modulus, loss modulus, and tan delta ratio (glass transition temperature) are 53.94°C, 67.27°C and 83.33 °C, respectively. Figures 18 and 19 show the TGA and DMA results for the 300% Cu laminate, respectively. The glass transition temperature was found to be 85.07 °C These values are relatively higher compared to the Freeman and Epoxies glass transition temperatures.

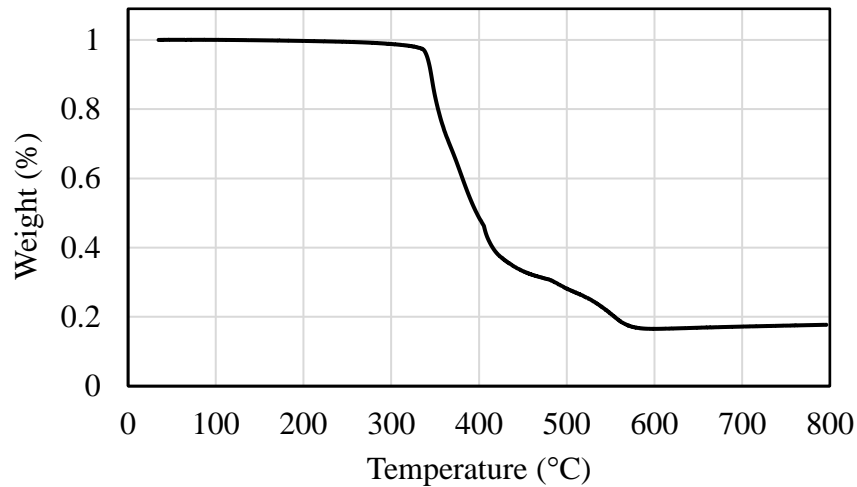


Figure 17: 20% Cu/ RIMR 135+RIMH 137 laminate (TGA test)

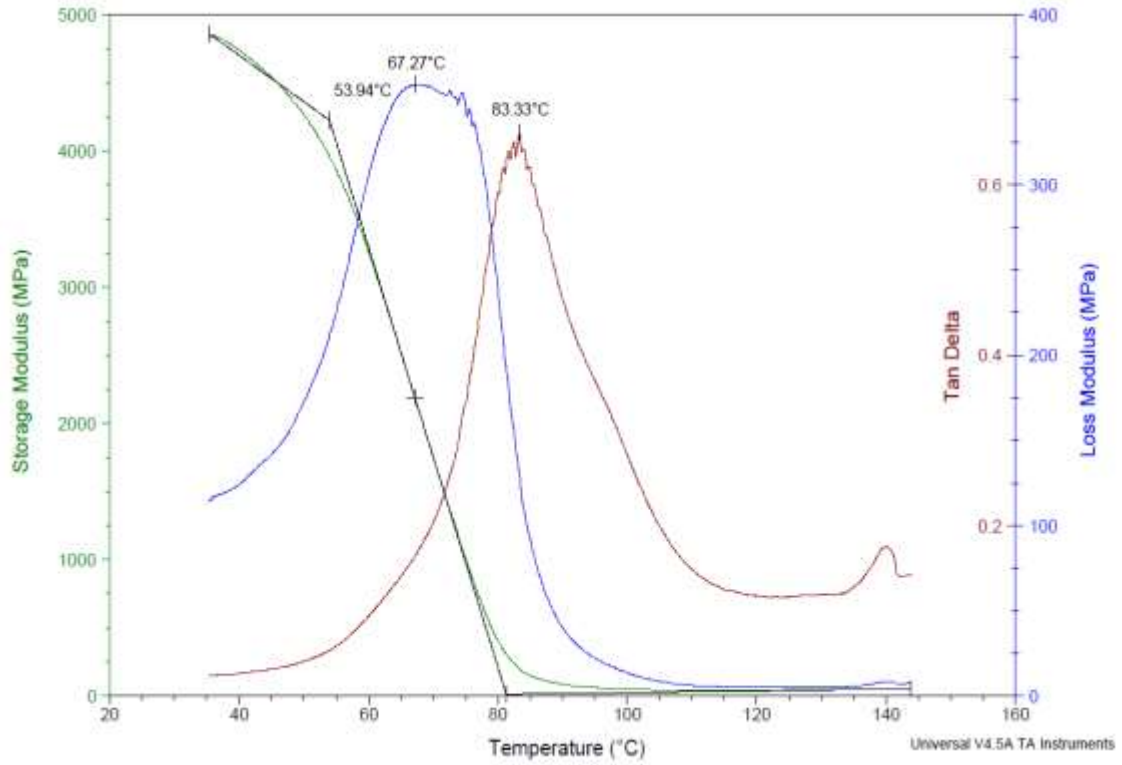


Figure 18: 20% Cu/ RIMR 135+RIMH 137 laminate (DMA test)

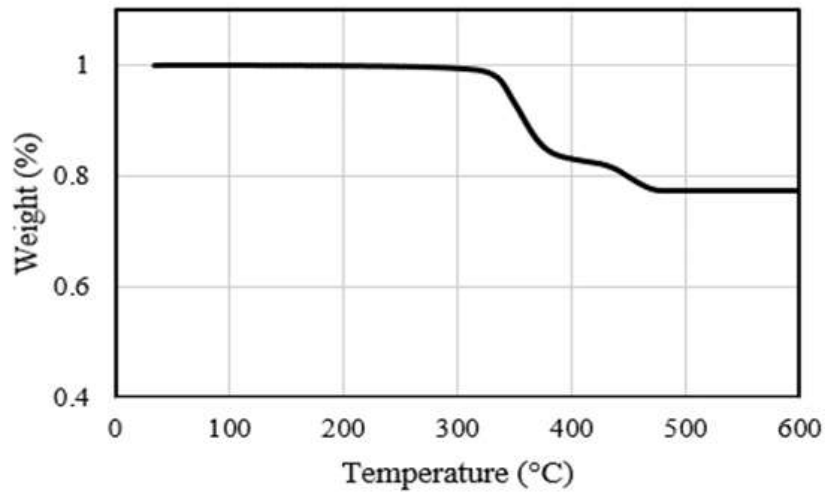


Figure 19: 300% Cu/ RIMR 135+RIMH 137 laminate (TGA test)

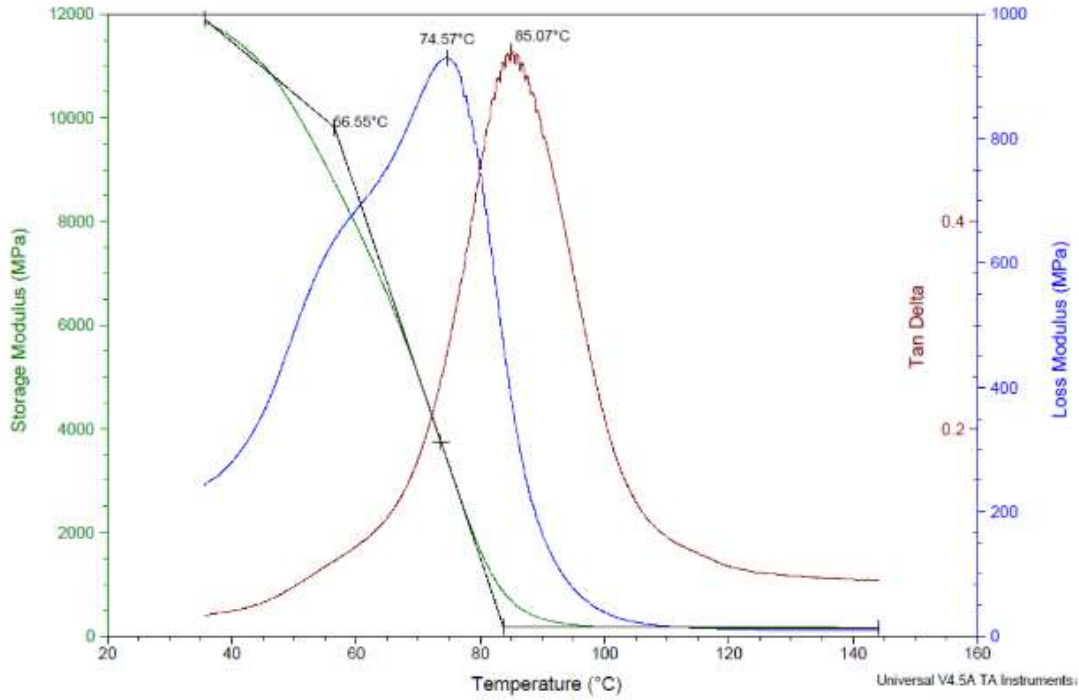


Figure 20: 300% Cu/ RIMR 135+RIMH 137 laminate (DMA test)

Thermal conductivity values for different laminates are summarized in Table 11 below. Freeman and Epoxies laminates were shown to have very similar thermal conductivity values, while a significant increase was shown in copper and graphite laminates.

Table 11: Thermal conductivity values for different laminates

Material	Thermal conductivity (W/m·K)	Density (kg/m ³)
Freeman laminate	0.85 ± 0.01	1.495
Epoxies laminate	0.99 ± 0.02	1710
600 weight % Cu/ RIMR 135 + RIMH 137	2.09 ± 0.01	4093
35 weight % graphite/ RIMR 135 + RIMH 137	1.86 ± 0.03	1606
20 weight % graphite flakes + 15 weight % / RIMR 135 + RIMH 137	1.47 ± 0.05	1606

5.2 Microstructure morphology of the composite laminates

Figures 21 a) and b) show the SEM images of the Freeman laminate. Both figures indicate relatively tightly packed aluminum particle clusters of irregular shapes and sizes. It can be observed that the particles are uniformly distributed across the laminate and that there is no discernable sedimentation occurring.

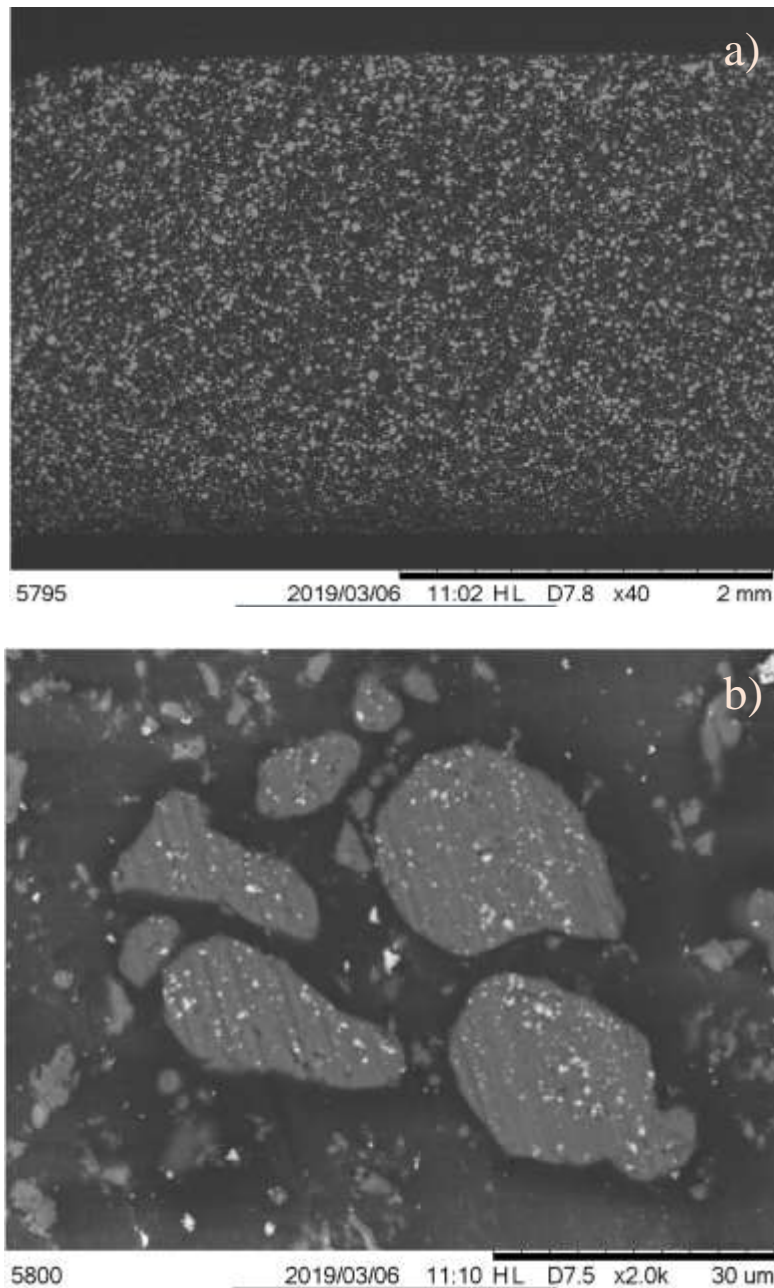
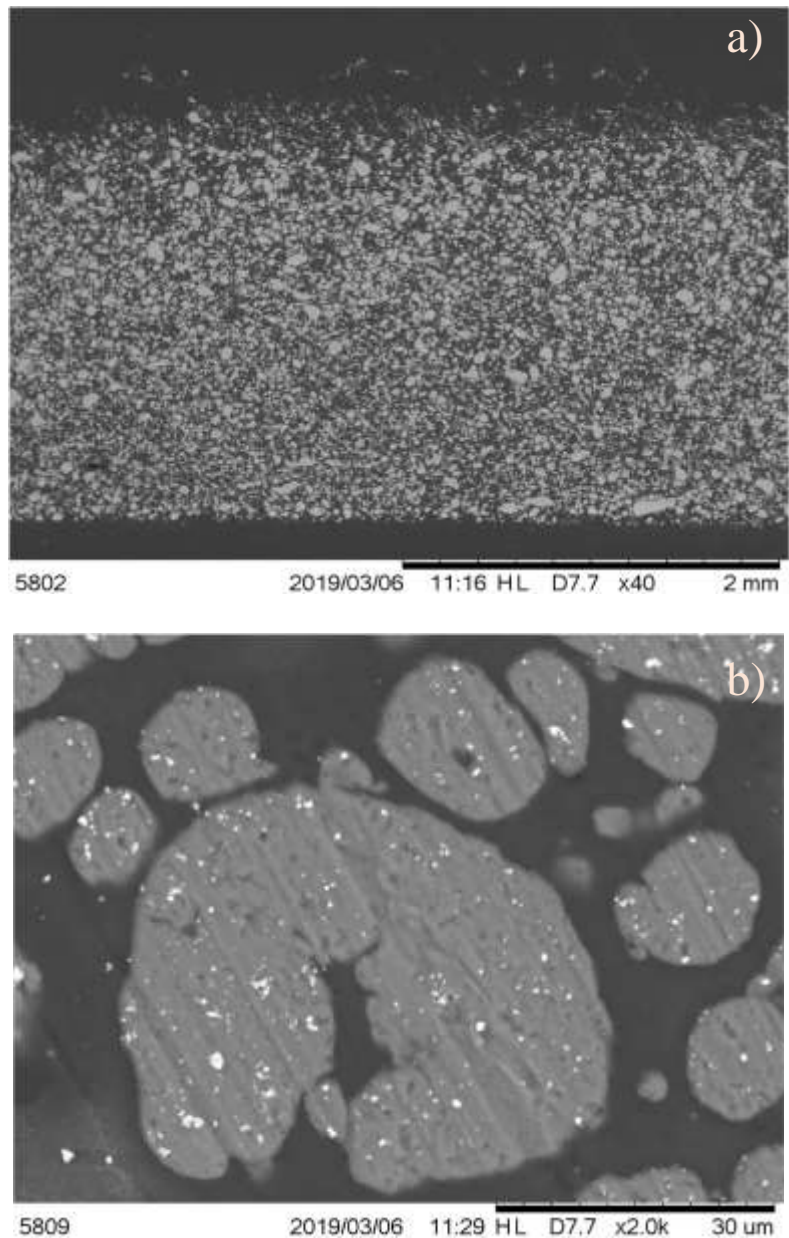


Figure 21: a) Freeman laminate SEM (1), b) Freeman laminate SEM (2)

Figures 22 a) and b) show the resulting SEM images of Epoxies laminate. Results indicate a noticeably higher content of aluminum particles as compared to SEM results of the Freeman laminate in Figures 21 a) and b). Some relatively insignificant sedimentation occurs at the bottom of the laminate, since the aluminum particles at the surface seem to be more dispersed.



SEM images of the 20% Cu laminate are shown in Figures 23 a) and b). It is evident from Figure 23 a) that the copper particles were not uniformly distributed throughout the laminate, but rather

clustered in one layer at the top of the laminate, whereas the epoxy, with a very few Cu particles, was sedimented at the bottom.

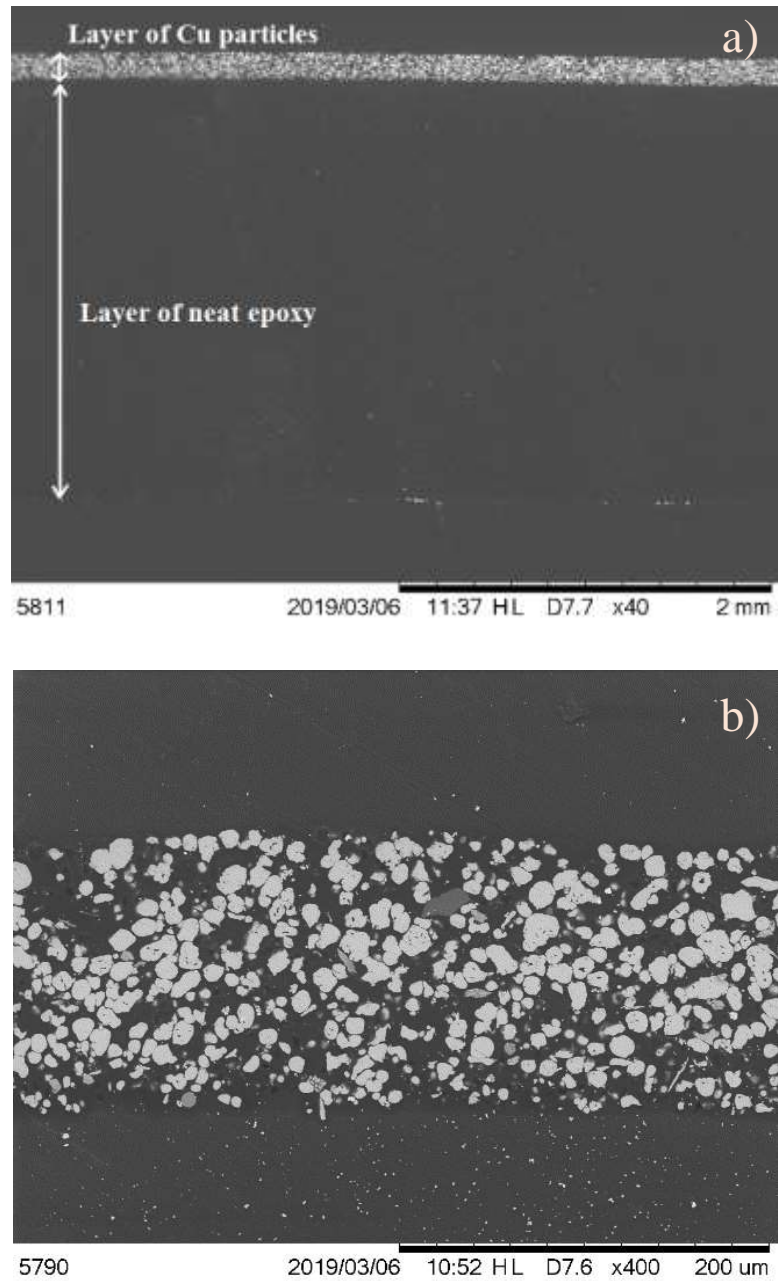


Figure 23: a) 20% Cu/ RIMR 135 + RIMH 137 SEM (1), b) 20% Cu/ RIMR 135 + RIMH 137 SEM (2)

Resulting SEM images of 300% Cu are shown in Figures 24 a) and b). It can be observed from Figure 24 a) that there is a significant neat epoxy layer on top of the laminate. This means that copper sedimentation has occurred and that a higher concentration must be used to make the laminate more uniform and more copper-dense so that very minimal amount of sedimentation would occur. Therefore, the Cu weight percentage was increased to 500%. Resulting SEM images are shown in Figures 25 a) and b).

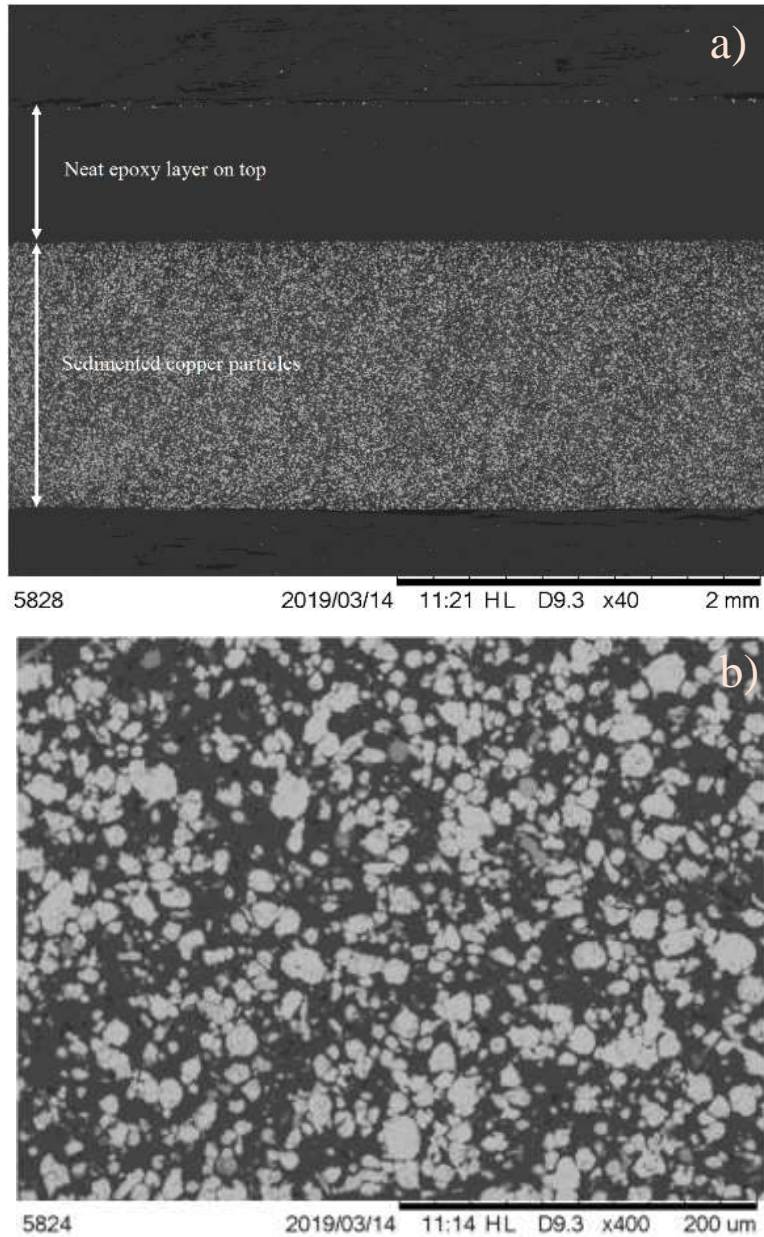


Figure 24: 300% Cu/ RIMR 135 + RIMH 137 SEM (1), b) 300% Cu/ RIMR 135 + RIMH 137 SEM (2)

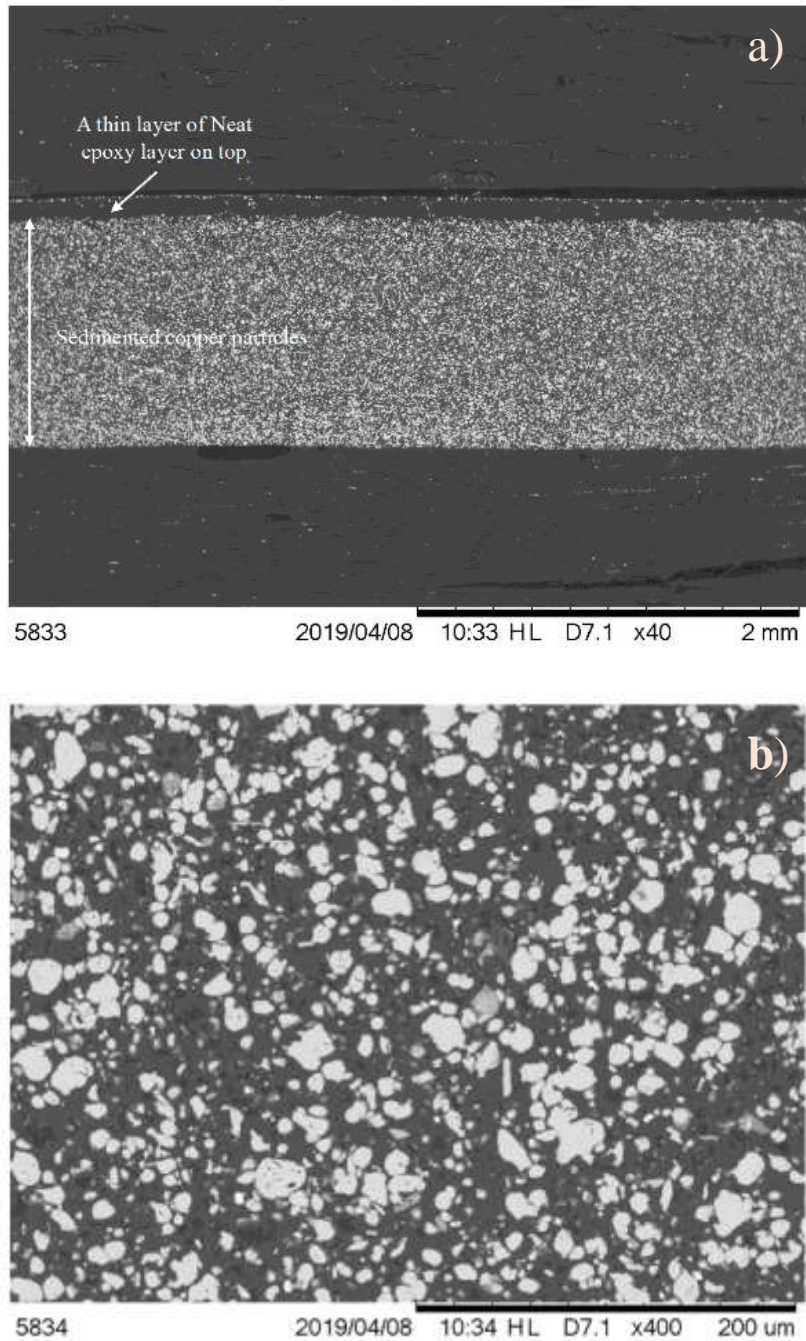


Figure 25: a) 500% Cu/ RIMR 135 + RIMH 137 SEM (1), b) 500% / RIMR 135 + RIMH 137 SEM (2)

In comparison to Figure 24 a), it can be clearly observed on Figure 25 a) that there is much less epoxy at the top of the laminate. This means that the weight increase of Cu indeed reduced the Cu sedimentation, but there were also issues in manufacturing the laminate. The more copper

was added, the harder it was to mix it in with the resin. In attempt to remove the remaining epoxy layer and completely reduce and remove the sedimentation occurrence, the 600% Cu laminate was fabricated. Resulting SEM images are shown below:

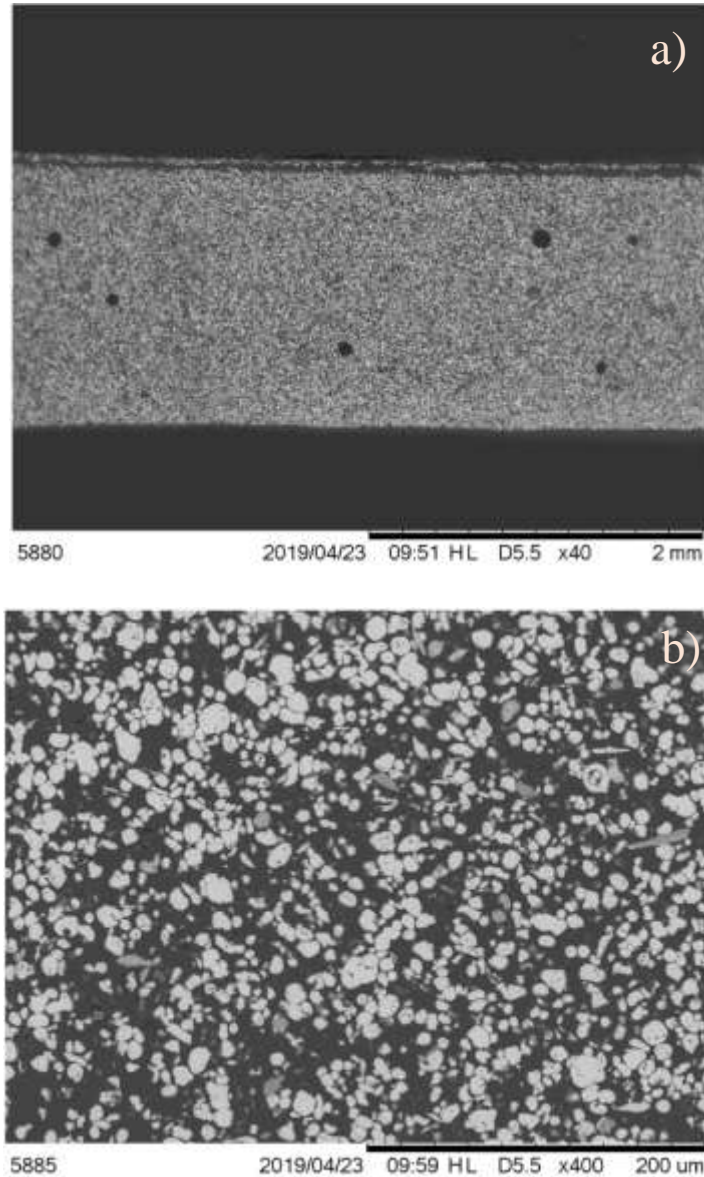
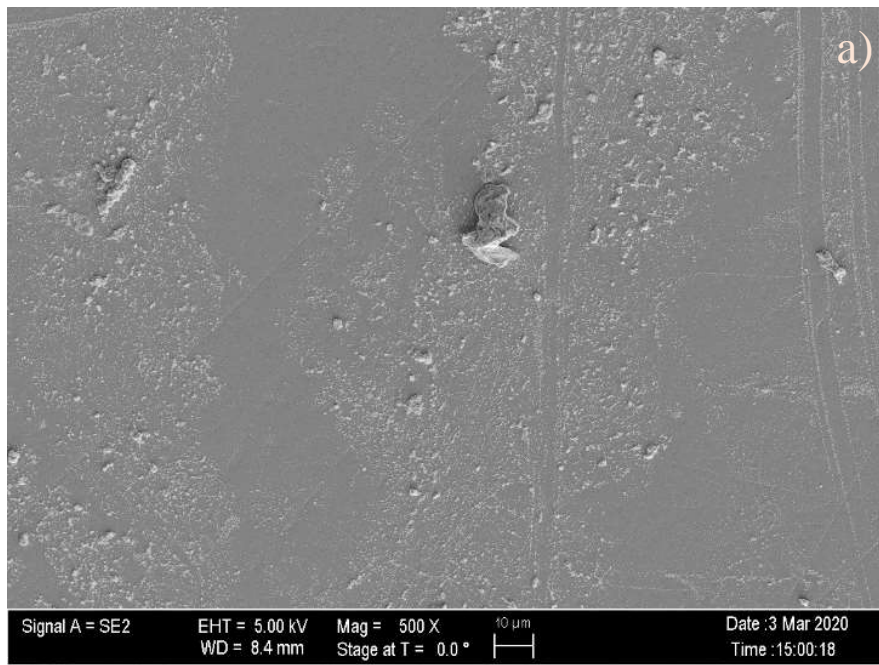


Figure 26 a) 600% Cu/ RIMR 135 + RIMH 137 SEM (1), b) 600% / RIMR 135 + RIMH 137 SEM (2)

It can be observed that SEM image of 600% Cu has almost no Cu-free epoxy layer on the top. The Cu sedimentation is significantly reduced from that shown in Figure 24 a). However, several medium to large voids have occurred in the laminate, meaning that the copper particles were

clustered and not well mixed with the resin, causing some parts of the laminate to be entirely without Cu particles. This was a somewhat expected result since mixing 500% Cu with the resin was difficult due to the large amount of Cu powder, so when the weight was increased by additional 100% the mixing process became even more difficult. That resulted in having some copper particles clustered and not well distributed throughout the laminate.

Figures 27 a) and b) show a x500 magnification of 7 weight % and 14 weight % graphite laminates, respectively. It appears that the graphite flakes are more uniformly dispersed in the 14% laminate, but some filler agglomerations are occurring in both laminates. Closer inspection at x2500 shows that both laminates, indeed, have a non-uniform distribution and agglomerations across the laminate. This comparison is shown in Figures 28 a) and b).



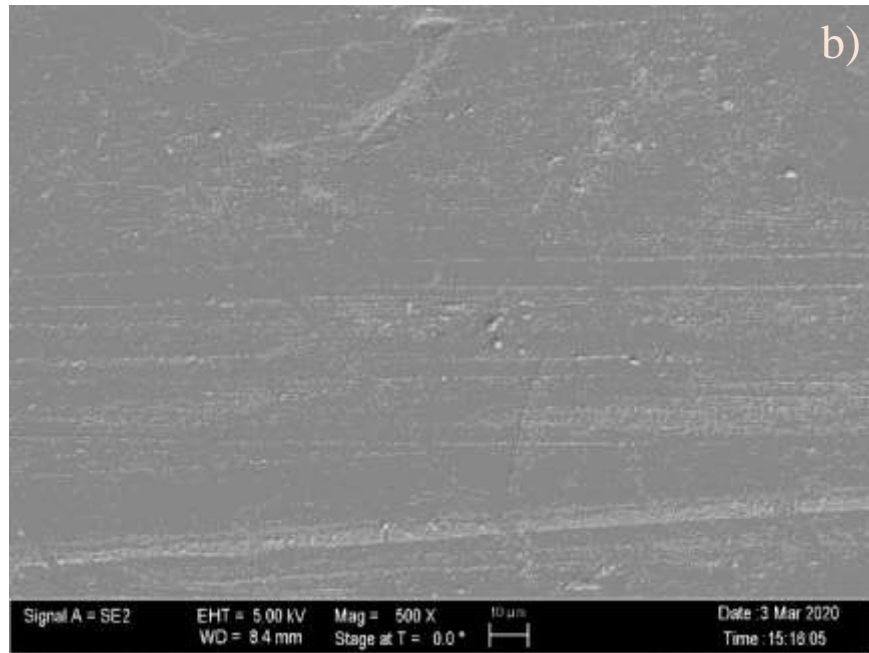
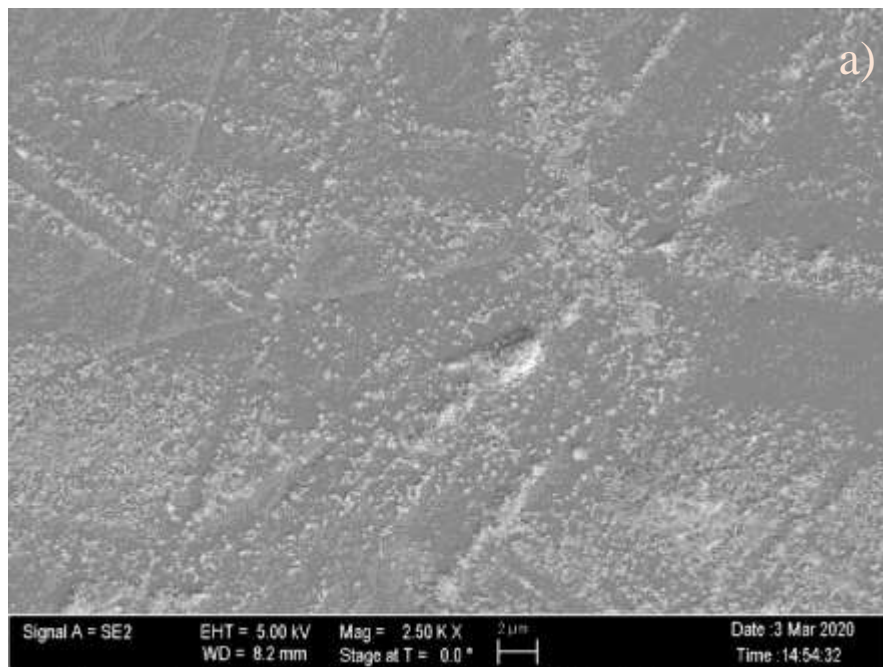


Figure 27: a) 7% graphite/ RIMR 135 + RIMH 137 at x500, b) 14% graphite/ RIMR 135 + RIMH 137 at x500



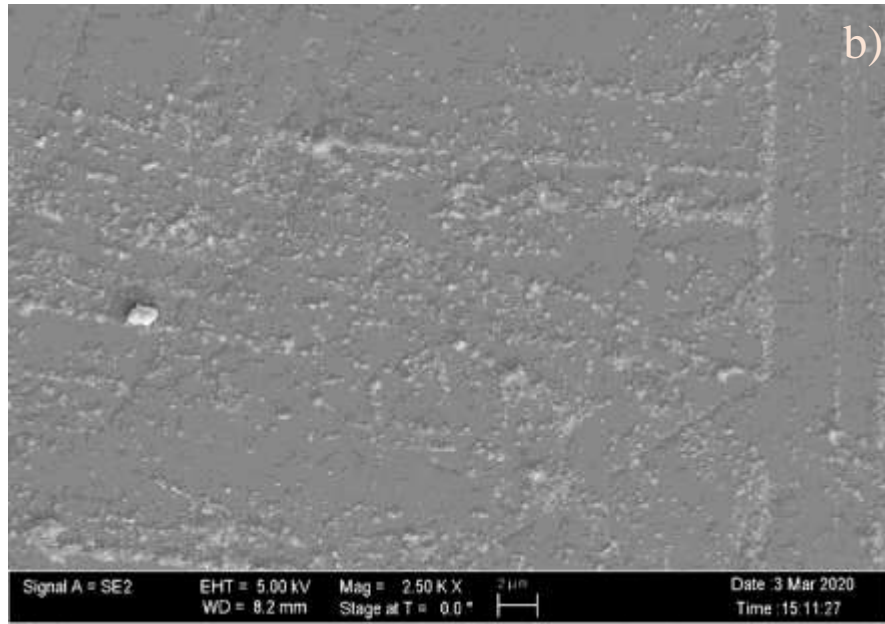
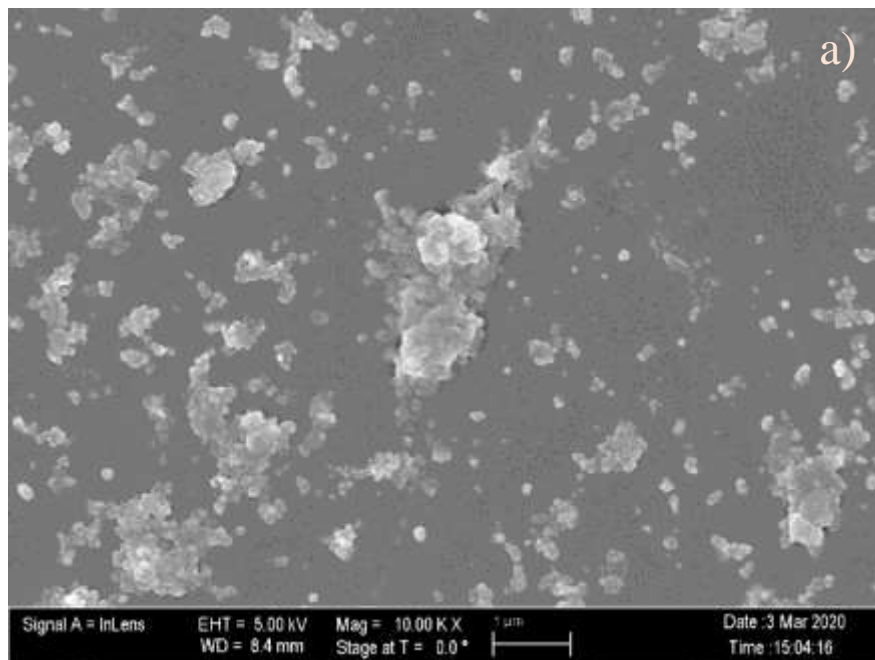


Figure 28: a) 7% graphite/ RIMR 135 + RIMH 137 at x2,500, b) 14% graphite/ RIMR 135 + RIMH 137 at x2,500

Agglomerations present in both laminates vary in size, shape and location. Figures 28 a) and b) show that within an area of $50\mu\text{m}^2$ the size of the graphite flake clusters range between 0.1 and $5\mu\text{m}$. Larger clusters are present in the 14% graphite laminate, as shown in Figure 29 b).



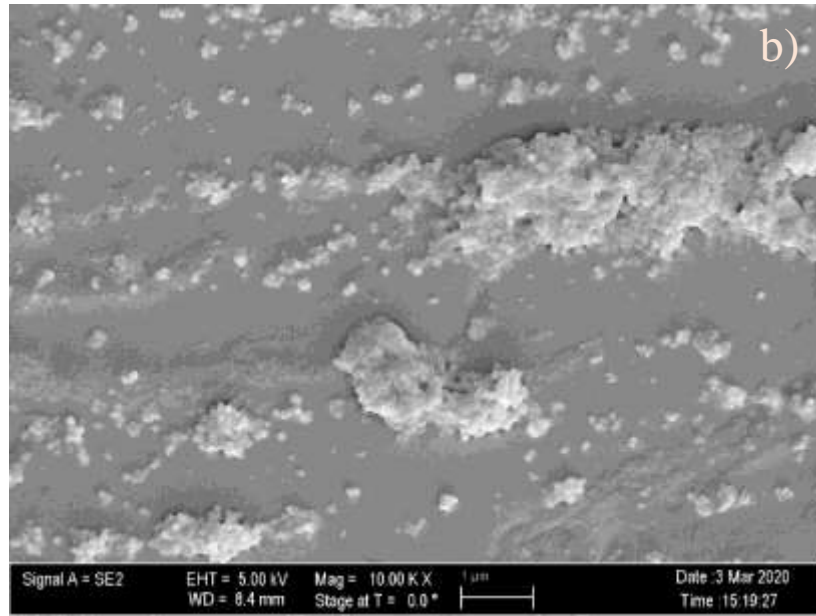


Figure 29: a) 7% graphite/ RIMR 135 + RIMH 137 at x10,000, b) 14% graphite/ RIMR 135 + RIMH 137 at x10,00

The issue of agglomeration was also present in other laminates, but to different extents. 20% graphite laminate has a very evident separation of graphite flakes and epoxy, as shown in Figure 30 a). Side by side comparison with a 35% graphite laminate (Figure 30 b)) shows that more agglomeration was present in the 21% laminate, which resembles the distribution of Cu shown in Figures 21-26. Larger Cu content provided a much more uniform distribution throughout the laminate, but the effect of sedimentation and agglomeration was inevitable. Similarly, larger graphite content still creates agglomerations throughout the laminate, but they are not as prominent as in the smaller weight percentage laminates because the particles are packed more tightly. Furthermore, it is evident from Figure 30 a) that with a smaller graphite weight percentage there are much larger neat epoxy areas throughout the laminate.

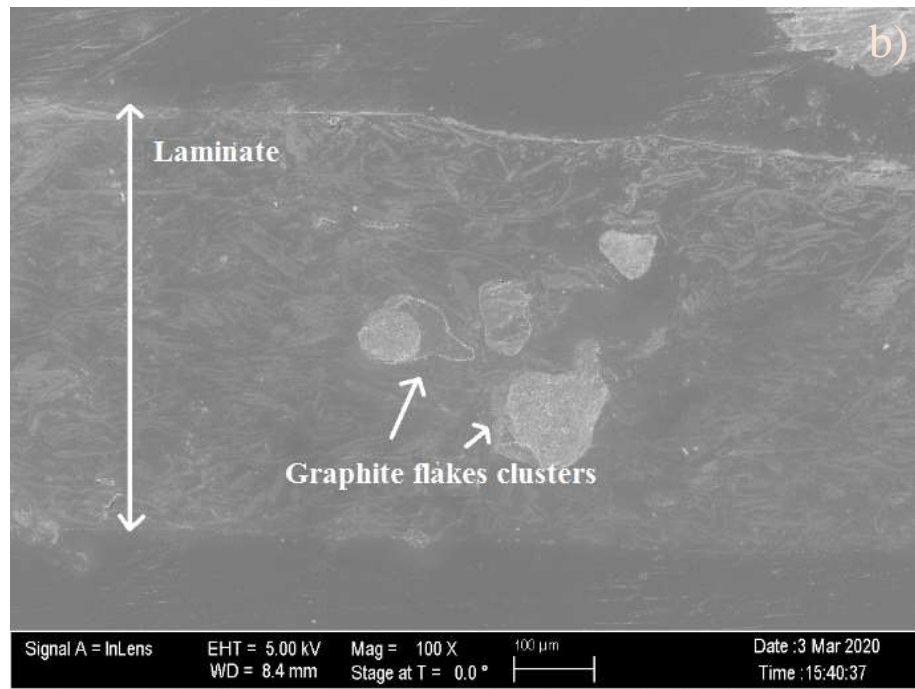
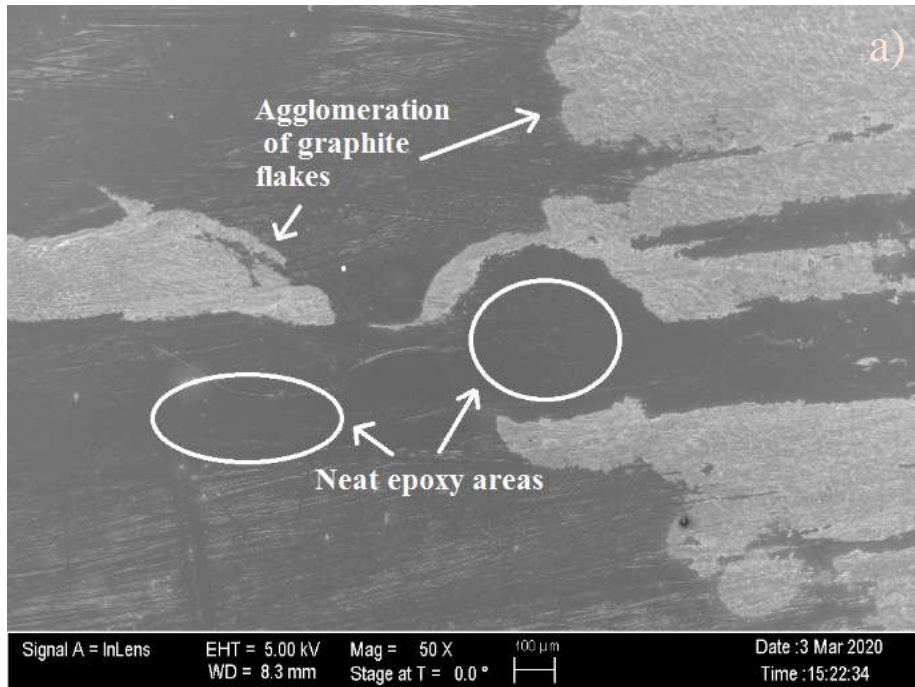


Figure 30: a) 20% graphite/ RIMR 135 + RIMH 137 at x50, b) 35% graphite/ RIMR 135 + RIMH 137 at x100

Closer inspection of both laminates (Figures 31 a) and b)) show that, indeed, larger weight percentage of graphite provided better filler distribution throughout laminate since neat epoxy

areas are significantly smaller and less frequent in a 35% graphite laminate. However, the graphite flakes are still not evenly distributed and are concentrated within the large clusters. Figures 32 a) and b) shows different irregular agglomerations in both 20% and 35% graphite laminates, respectively.

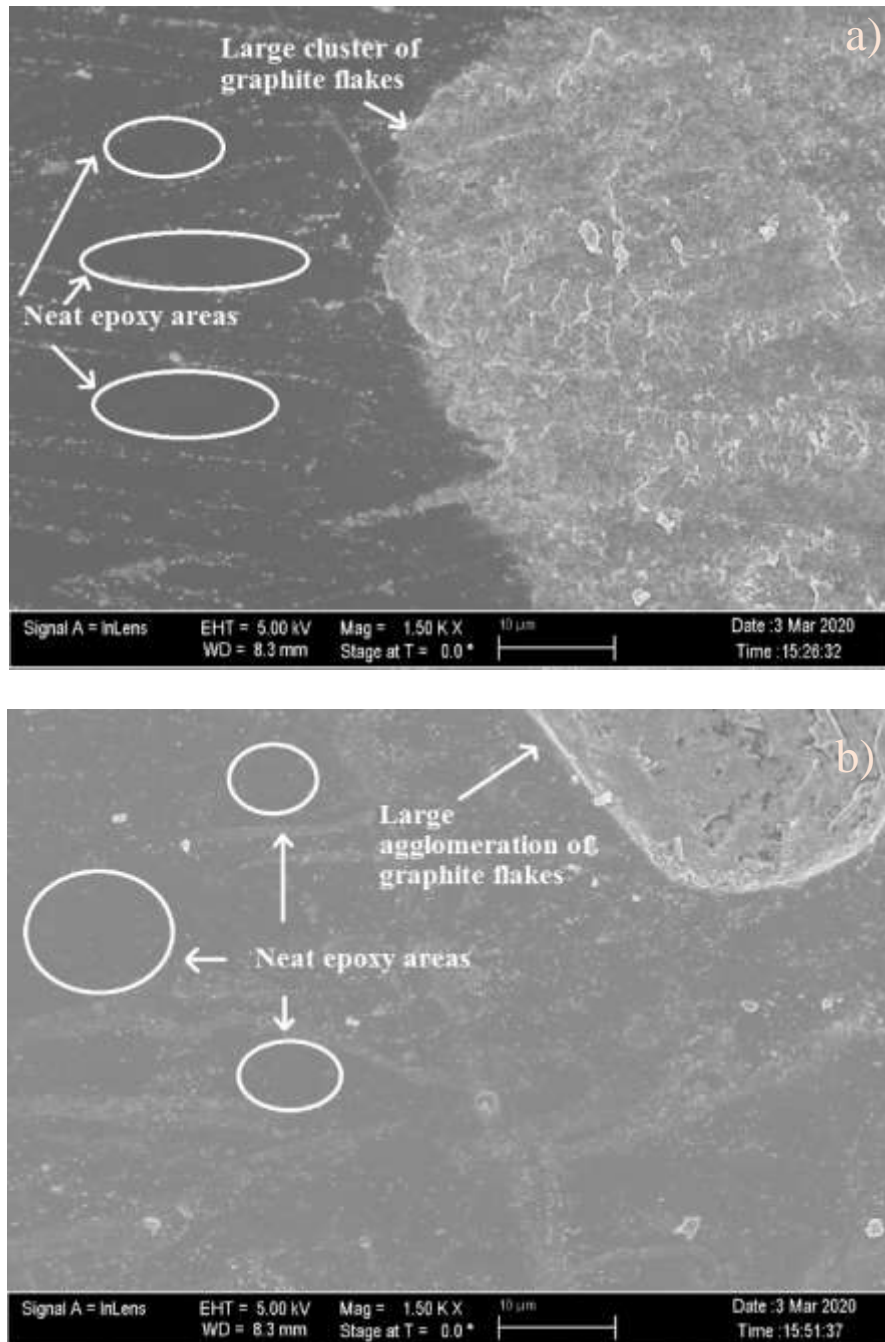


Figure 31: a) 20% graphite/ RIMR 135 + RIMH 137 at x1,500, b) 35% graphite/ RIMR 135 + RIMH 137 at x1,500

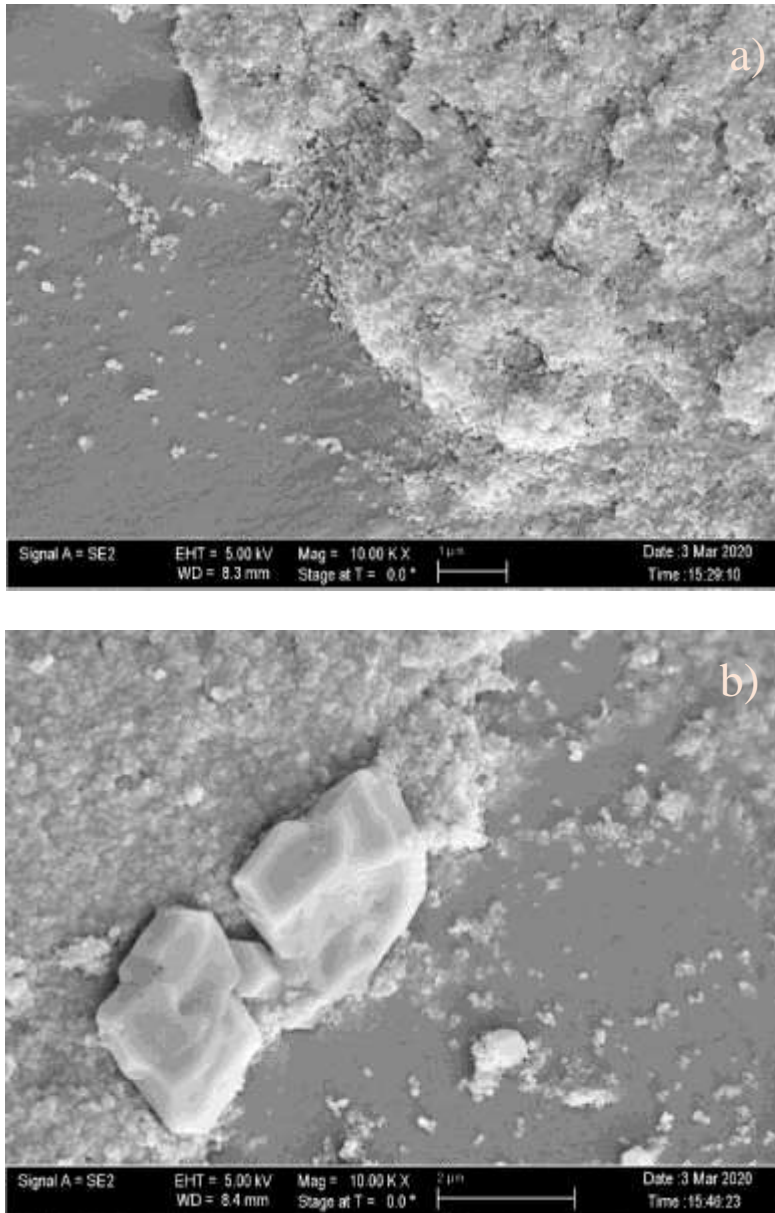


Figure 32: a) 20% graphite/ RIMR 135 + RIMH 137 at x10,000, b) 35% graphite/ RIMR 135 + RIMH 137 at x10,000

Figures 33 a) and b) show a side-by-side comparison between hybrid graphite laminates, 15 weight % of graphite flakes + 5% of graphene nano powder and 30%+5% hybrid, respectively. The goal was to improve structural network of the laminate by introducing second thermally conductive filler material which would contribute to the overall improvement in material distribution throughout the laminate. As observed from the Figures 33 a) and b), it is evident how both laminates still have a noticeable amount of filler material agglomerations.



Figure 33: a) 15+5% graphite/ RIMR 135 + RIMH 137 at x100, b) 30+5% graphite/ RIMR 135 + RIMH 137 at x100

Observing these laminates at higher magnifications allowed for a better understanding of how the two filler materials interact with each other and whether the observed agglomerations show a network structure or if the materials are randomly dispersed. A very interesting effect can be observed from Figures 34 a) and b). Figure 34 a) represents the 15+5% hybrid laminate, where the filler material seems to agglomerate into strips and form a somewhat repeating pattern throughout the laminate. The graphite flakes and graphene nano powder cannot be easily differentiated from this image, which can be an indicator that they formed a good network within the clusters. Nevertheless, the overall material distribution throughout the laminate is somewhat poor. Figure 34 b) shows a 30+5% hybrid laminate with a much better material dispersion.

However, lighter contrast on SEM images represents smaller particles and a significant constant difference can be observed. Hence, it becomes evident that graphite flakes and graphene nano powder have separated and formed individual clusters, as identified and marked on Figure 34 a). Figures 35 a) and b) also support these observations and show the composition of these laminates at higher resolution, where it becomes even more apparent that a significant separation of the filler materials in the 30+5% laminate occurs, whereas the 15+5% has very little to no separation, but the overall laminate quality is compromised.

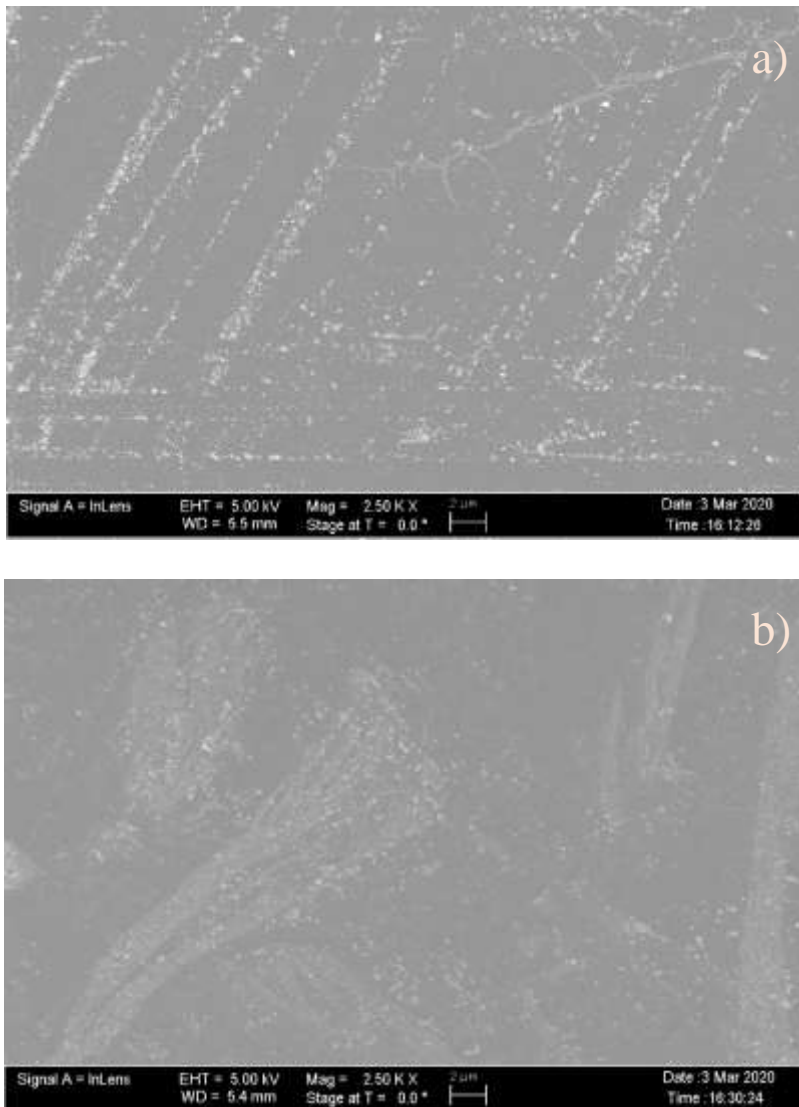


Figure 34: a) 15+5% graphite/ RIMR 135 + RIMH 137 at x2,500, b) 30+5% graphite/ RIMR 135 + RIMH 137 at x2,500

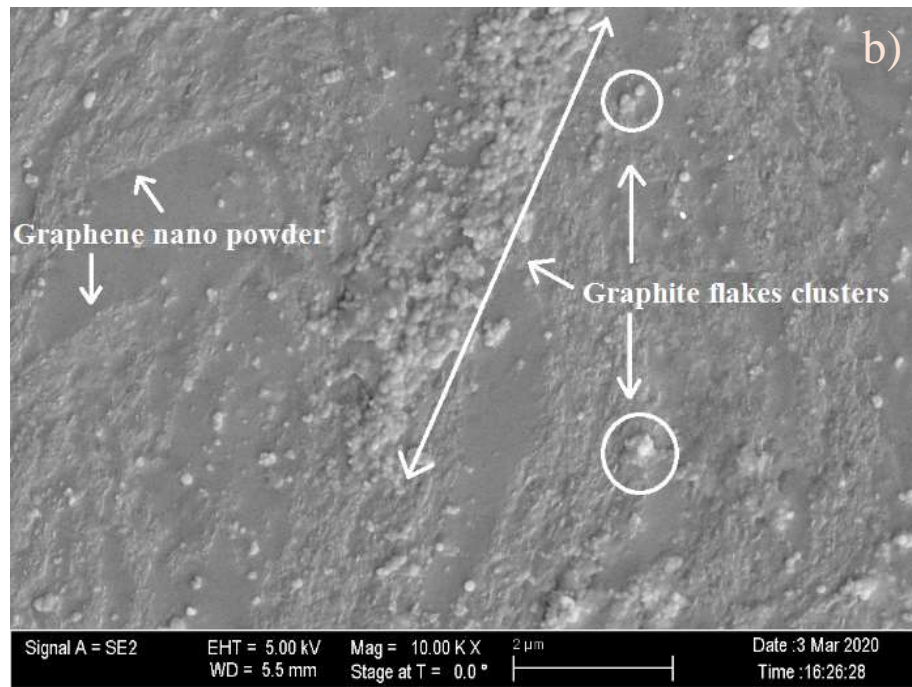
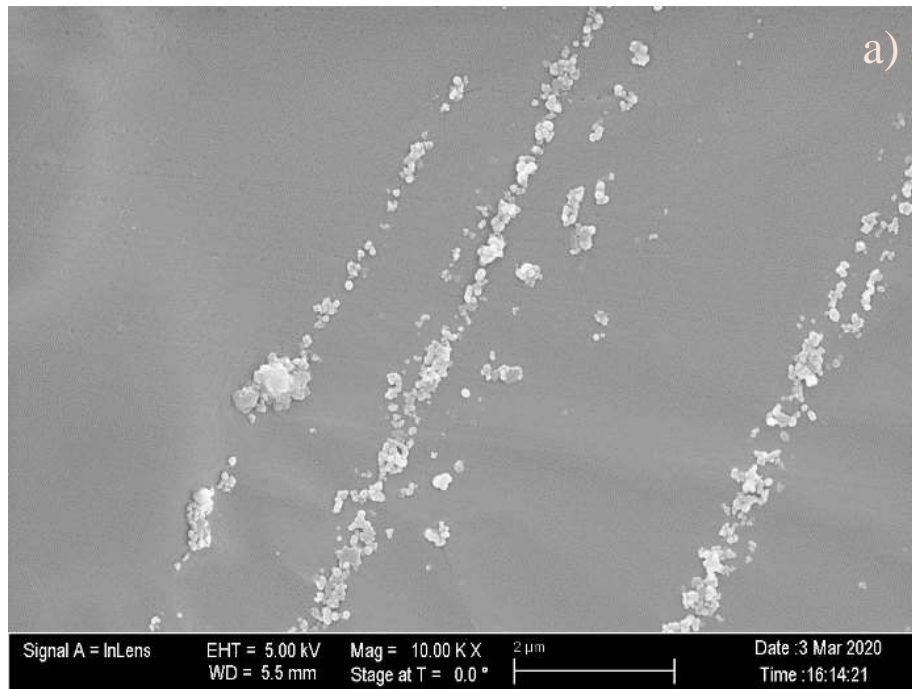


Figure 35: a) 15+5% graphite/ RIMR 135 + RIMH 137 at x10,000, b) 30+5% graphite/ RIMR 135 + RIMH 137 at x10,000

An intuitive conclusion from these observations would be that a smaller graphite flakes to graphene nano powder ratio (3:1) is more effective in creating a better network, but that the

higher overall ratio (6:1) contributes to a better material dispersion. However, if the amount of material in the 3:1 ratio was increased to, for example, 30% graphite flakes and 10% GNP, the laminate would be much more difficult to fabricate due to the issues described in the Section 3. of this chapter. Larger filler material content (35% was the largest overall graphite weight percentage fabricated) was difficult to mix with epoxy and resulted in a high viscosity paste-alike material that couldn't be properly casted. Hence, the overall 40% weight content of graphite would be even more difficult to fabricate.

5.3 Mechanical properties of the composite laminates

Flexural stiffness, strength and strain to failure ratio of the laminates containing graphite were determined by a flexural test (i.e., three-point bending test). Table 12 represents the summary of average values found for the graphite laminates.

Table 12: Summary of graphite laminates flexural test results

Graphite Weight %	Average Flexural Strength [MPa]	Average Flexural Stiffness [GPa]	Average Strain to Failure
7	63.15 ± 4.19	3.90 ± 0.37	0.02
4	57.30 ± 8.31	4.46 ± 0.62	0.02
20	50.55 ± 11.15	4.32 ± 1.05	0.01
35	63.45 ± 3.59	5.76 ± 0.64	0.04
15+5	67.12 ± 7.08	4.51 ± 0.80	0.03
30+5	76.41 ± 2.74	5.21 ± 0.73	0.03

It can be observed from the above table that the lowest flexural strength occurs in the 20% graphite flakes laminate. The main reason behind this result is most likely the poor distribution of graphite particles throughout the laminate, as shown in Figure 30. Furthermore, high standard deviation indicates that there were varying results among the laminate samples, which proves that poor material dispersion contributed to nonhomogeneous properties. The highest flexural strength among the graphite flakes laminates was achieved by 35% laminate, indicating that the higher graphite content improves overall flexural strength. This observation is supported by the hybrid laminate results as well. Significantly higher flexural strength value is achieved in the

30+5% hybrid laminate. Comparison between the same overall filler material weight percentages shows that addition of graphene nano powder improves flexural strength. For example, the flexural strength for the 20% and 35% filler content were increased by ~17MPa and ~13MPa, respectively. However, the overall flexural strength value of the neat epoxy laminate, 105 MPa, is significantly compromised by the addition of graphite and graphene. The strength values of the composites were almost twice as smaller. In comparison to Freeman and Epoxies laminates, the graphite composites performed similarly. Flexural strength of the Freeman laminate is approximately 45MPa, and 62MPa of the Epoxies laminates, according to the material data sheets. Evidently, the strength values for 35% graphite and hybrid laminates are significantly higher.

Flexural stiffness values experienced the same trend as the strength. Increase in graphite/graphene content increased the flexural stiffness of the laminate, with 35% graphite laminate achieving the highest value. Average strain to failure values ranged between 0.01 to 0.04, with the highest value achieved by the 35% laminate. The lowest value, 0.01, achieved by the 20% laminate, again shows the consequences of poor dispersion and nonuniform material distribution. This trend also shows that the addition of larger content of filler material contributes to the increase in the laminate's overall strain to failure ratio.

Chapter III: Design and 3D Printing of the Heat Exchanger and Flow Channels

1. Objective

This chapter will describe the process of designing and 3D printing models of a compact heat exchanger and its internal flow channels that circulate the fluid to be cooled. The procedure starts with designing 3D models of the heat exchanger and then flow channels separately, so that the polymer heat exchanger can be easily fabricated. The developed models were 3D printed and used to fabricate different silicone molds, later used for polymer heat exchanger fabrication by casting as described in Chapter 4.

2. Compact heat exchanger design

2.1 3D model of the compact heat exchanger

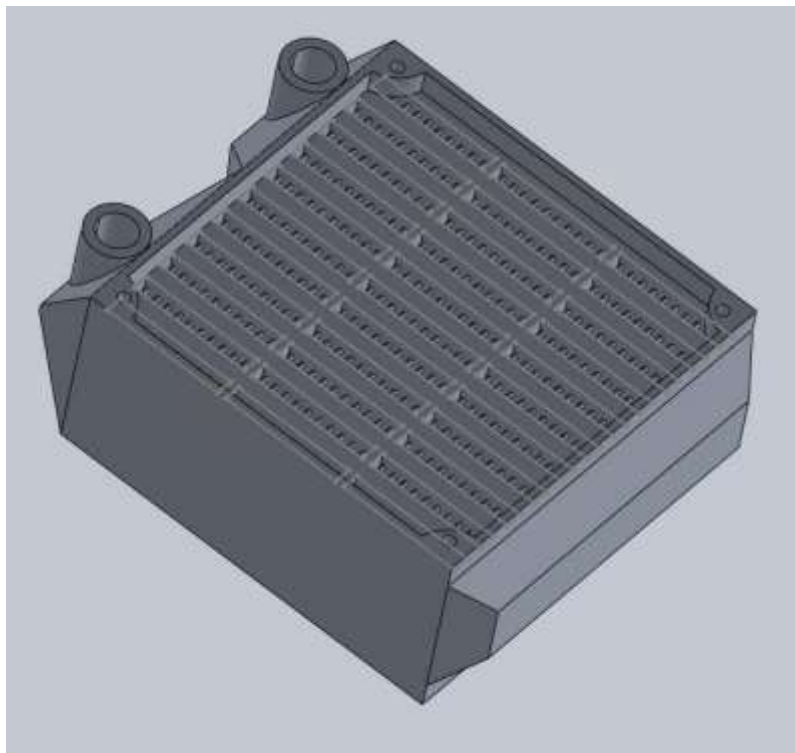


Figure 36: 3D model of the compact heat exchanger (isometric view)

A 3D model of the compact heat exchanger was initially developed by the Oak Ridge National Laboratory researchers in SolidWorks program, as shown in Figure 1. The dimensions of the designed device are 6in x 4in x 2in. The model represents a complete heat exchanger design with all the necessary components, including an inlet, an exit, and the internal flow channels. Flow channels of a heat exchanger are horizontal or vertical slots through which a hot air or other fluids to be cooled can flow. The reason for having flow channels in these devices is because their presence increases the surface-to-volume ratio, meaning that more areas of the device will be heated with the hot air, hence the heat transfer rate will be increased. Moreover, conventional heat exchangers further increase the heat transfer surface area by adding porous sections for cross flow in the space between the flow channel walls, instead of leaving it hollow. In this model, flow channels of the heat exchanger are fully designed along with the essential porous sections that will allow for the cross-air flow. This model is used to provide a general shape and dimensions of the polymer heat exchanger that will be fabricated, as well as to fabricate silicon molds used in the final stages of fabrication. Figures 37-42 below show additional dimensional characteristics of the model. All dimensions shown are in millimeters (mm).

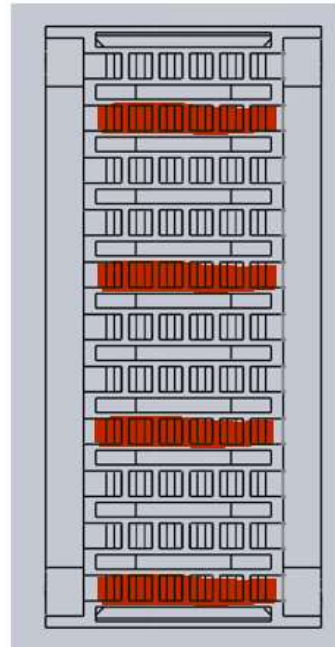


Figure 37: Cross-section view of the 3D heat exchanger model. 4 out of 11 flow channels are labeled in red.

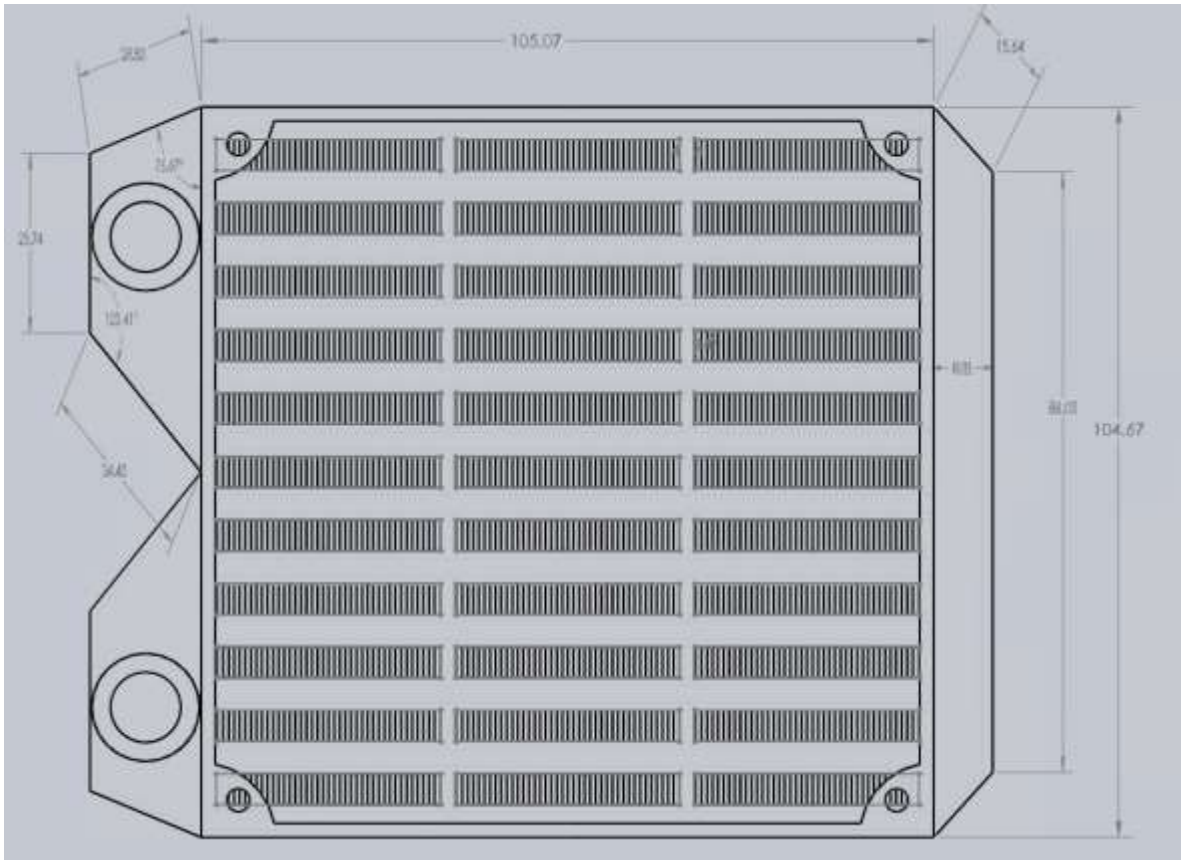


Figure 38: Heat exchanger dimensions

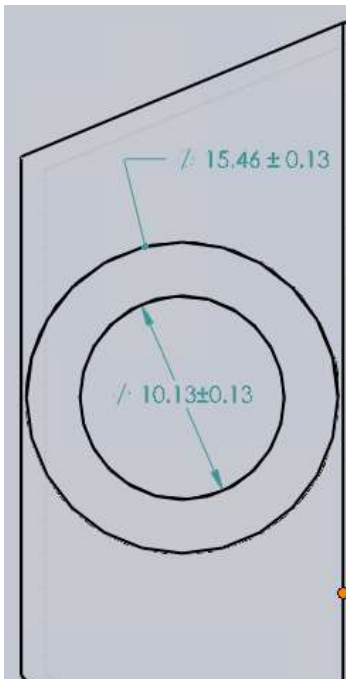


Figure 39: Inlet/outlet dimensions

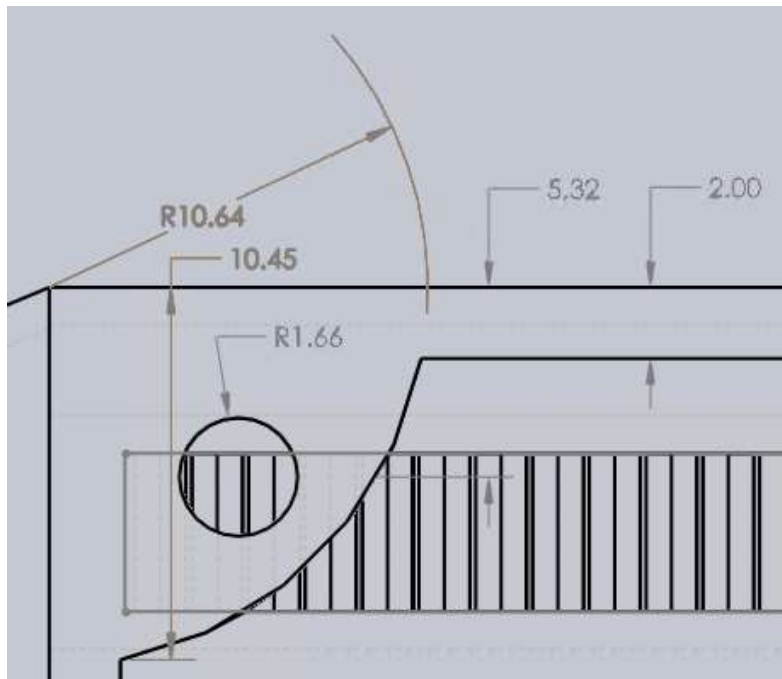


Figure 40: Inlet and wall thickness dimensions

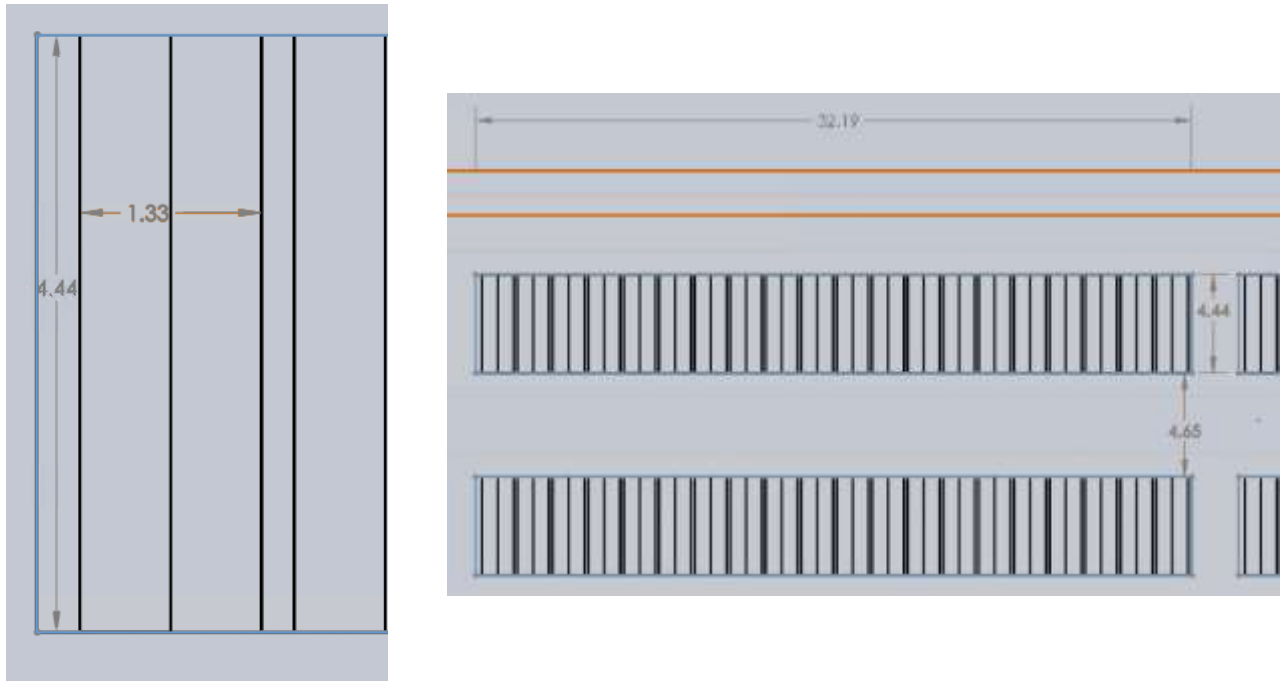


Figure 41: Dimensions of the flow channel grid within the heat exchanger

```

Mass properties of Epoxy heat exchanger
Configuration: Default
Coordinate system: -- default --

Density = 1.100 grams per cubic centimeter

Mass = 190.478 grams

Volume = 173.162 cubic centimeters

Surface area = 2832.649 square centimeters

Center of mass: ( centimeters )
X = -0.149
Y = 0.000
Z = 1.335

```

Figure 42: Mass properties of the heat exchanger model calculated through SolidWorks analysis tools if the model was made out of neat epoxy

2.2 3D model of the heat exchanger flow channels

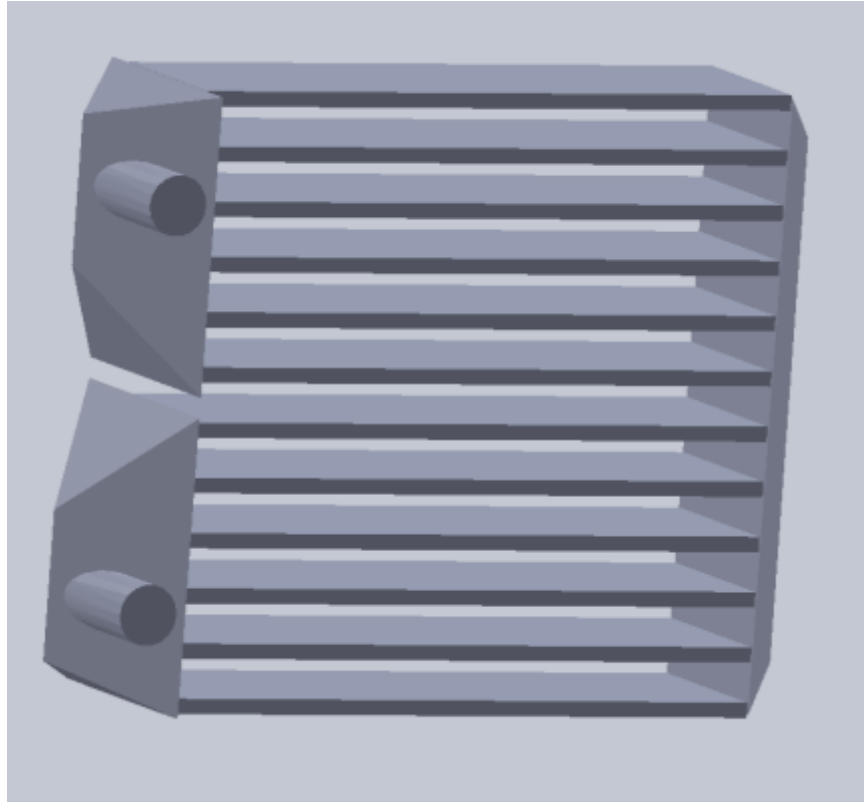


Figure 43: 3D model of flow channels

3D model of the heat exchanger flow channels was also developed in SolidWorks program. Dimensions of the model are 4in x 4in x 1.2in. There are 11 flow channels, and the dimension of each is 4in x 0.25in x 2in. Wall thickness of the flow channels and the outside walls is 0.1in. Flow channels are individually designed so that an expandable mold of this structure can be easily fabricated. The following Figures 44-48 show close-up details of this model and their dimensions, in mm.



Figure 44: Left side view

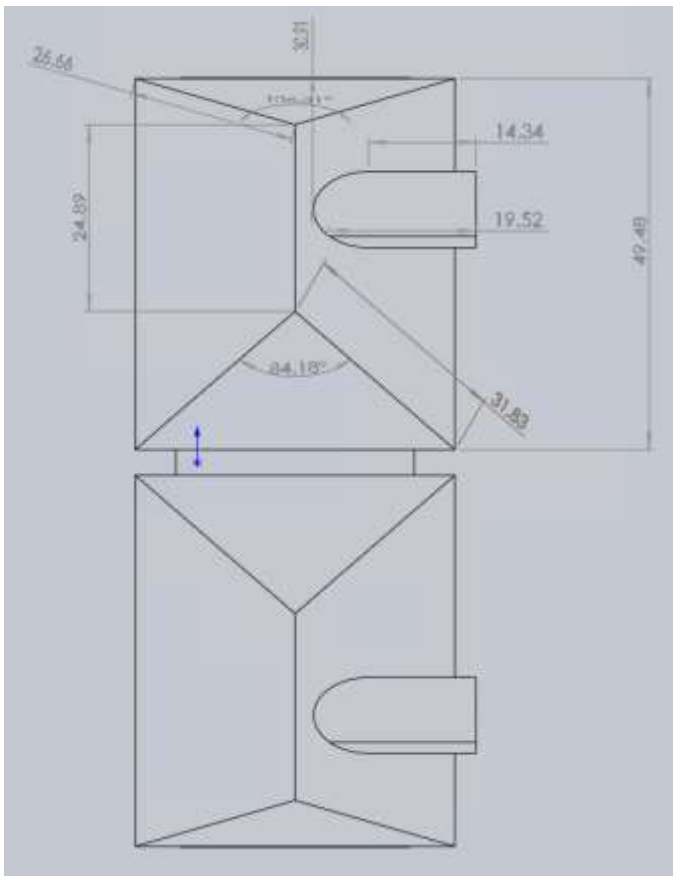


Figure 45: Top view

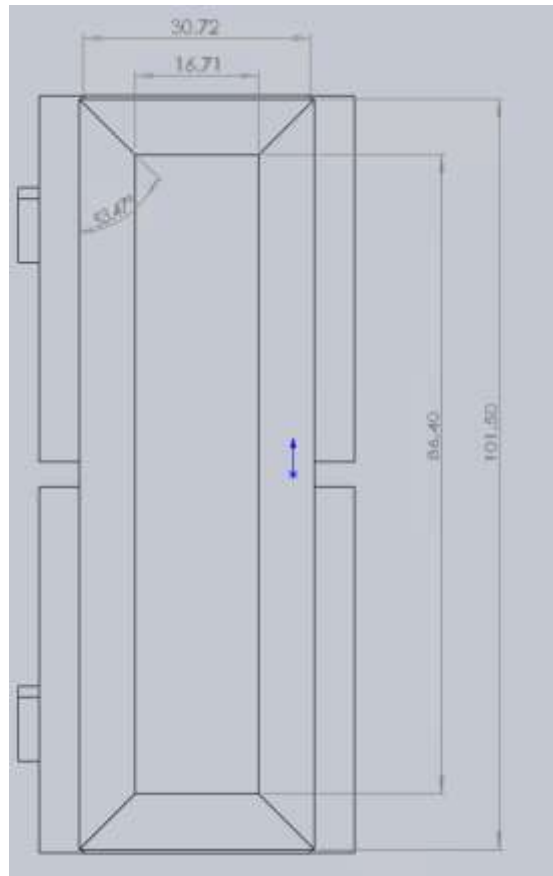


Figure 46: Bottom view

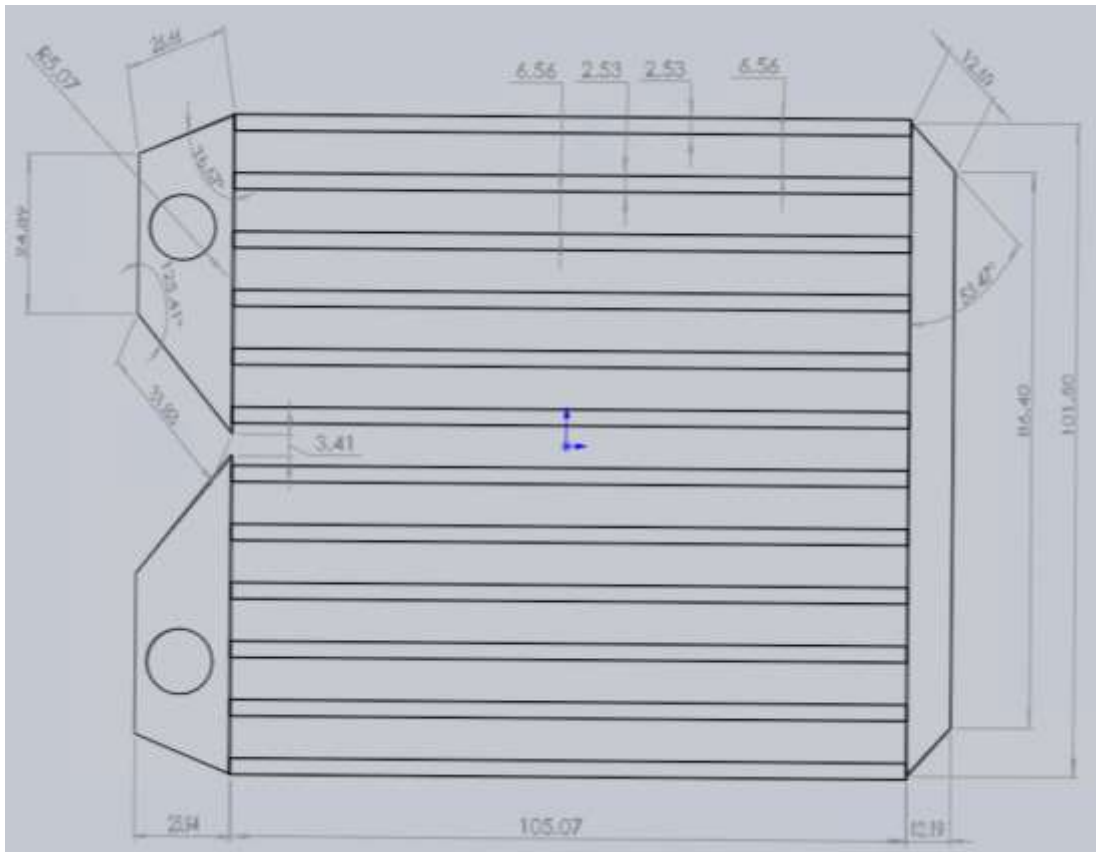


Figure 47: Flow channel dimensions

Mass properties of Heat exchanger flow channels
 Configuration: Default
 Coordinate system: -- default --

Density = 1.100 grams per cubic centimeter
 Mass = 121.930 grams
 Volume = 110.825 cubic centimeters
 Surface area = 997.008 square centimeters

Center of Mass: (centimeters)
 X = -0.189
 Y = 0.000
 Z = 1.325

Figure 48: Mass properties of the flow channels model calculated through SolidWorks analysis tools if the material of the model is neat epoxy

3. 3D printing of the heat exchanger and flow channels models

Both 3D models described in section 2.1 and 2.2 were printed at the OU Innovation Hub facility with ABS material. ABS (Acrylonitrile Butadiene Styrene) supports 3D printing applications at 210 °C - 250 °C and requires a heated printbed in order to prevent material cracking or deforming. ABS is a very durable material and suitable for prototyping new designs, which is also slightly flexible and heat resistant. Furthermore, ABS is an affordable material that has a large range of applications in different industries, such as production of pipes, electronic assemblies, and kitchen appliances. Great benefit of using ABS is that it can be sanded or glued together with other ABS 3D printed parts. One of the main characteristics of ABS is that it is a non-biodegradable plastic material. During the 3D printing process, it may create mild fumes if the operation temperature is very high. This material degrades if exposed to sunlight over a long period of time and is known to sometimes attract moisture from the ambient air. Despite these few disadvantages, it is one of the most commonly used 3D printing materials. Some properties of the ABS material are shown in Table 13.



Figure 49: Filaments of ABS material used in 3D printing (image courtesy to 3DPFB.com)

Table 13: Properties of ABS [17]

Specific gravity	1.06
Glass transition temperature [°F]	221
Heat deflection temperature [°F]	208
Tensile strength [psi]	6,600
Flexural strength [psi]	10,800
Shrink rate [in/in]	0.005-0.007

The entire heat exchanger model took 20 hours to print, whereas the internal flow channels model took around 12 hours. The end results are durable, somewhat flexible models that will be used in manufacturing corresponding molds for the heat exchanger fabrication.

There are no sudden steps in either final product, which occur when discontinuous forces are present. There are no dangerous sharp corners in either model, however, there are 90° internal and external corners and edges that may affect dimensional accuracy of the printed model, as shown in Figure 50.



Figure 50: 3D printed heat exchanger model. Some parts of the model that have 90° corners and edges are circled in red

Flow channel model has an opening that makes the model more prone to breaking. It is used for manufacturing silicone molds required for expandable flow channels fabrication. The red circled area in the Figure 51 shows a weak point of the model where a possible damage and breaking may occur since the top of that channel is not closed (circled in white). However, regular use of this product has not caused it any damages so far.



Figure 51: 3D printed flow channels. Part of the model that experiences the largest stress due to the top opening is circled in red.

Chapter IV: Fabrication of the Compact Polymer Heat Exchanger

1. Objective

This chapter describes the fabrication procedure of the polymer heat exchanger. 3D printed models discussed in Chapter III were used to fabricate silicone molds for heat exchanger and flow channels. The flow channels silicone mold was then used to fabricate expandable flow channels that can be melted and easily removed from the polymer heat exchanger, creating the structure of the conventional heat exchanger device. The polymer heat exchanger was fabricated by gravity casting. Polymer was poured over the expandable flow channels placed in the heat exchanger silicone mold and supported with a fixture. Once the polymer was cured, the expandable internal flow channels were removed, thus creating hollow flow channels inside the exchanger. This entire process is illustrated in Figure 52 below.

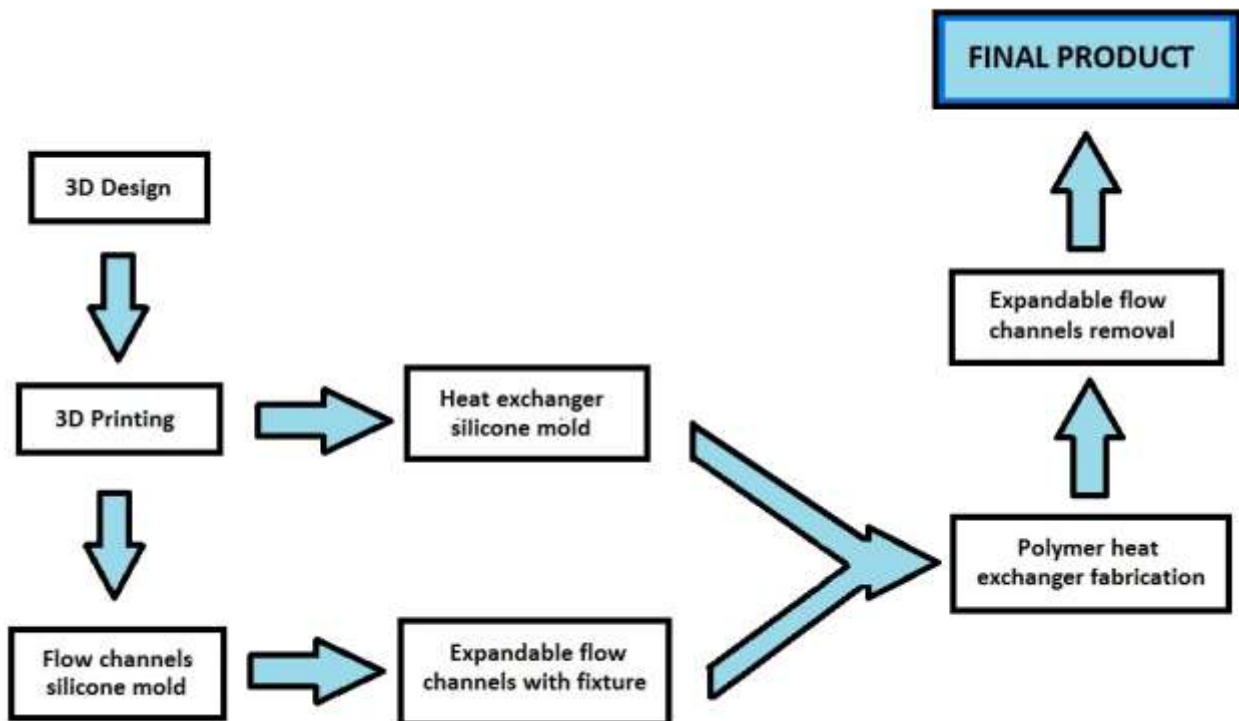


Figure 52: Design and fabrication of a compact polymer heat exchanger flowchart

2. Materials

AM 115T Translucent Silicone RTV Rubber by AeroMarine Products was used to fabricate silicone molds. This is a translucent, two-component silicone material that has very high tear strength and great dimensional stability. According to the technical data sheet, a general preparation procedure of this product is as follows: The mixing ratio of the two products shown in Figure 53 below is 10:1 by weight (must use a digital gram scale). An A amount of the Silicone RTV Rubber compound must be measured first. 0.1xA amount of the catalyst was then added in a clean container and mixed well until the mixture is uniform. The mixture is poured or left in the container to cure for 24 hours to get a desired silicone mold. ½” should be the minimum thickness of the mold; very thick molds have reduced resistance to tearing, whereas too thick molds have reduced flexibility. Properties of the cured silicone are collected from the product’s technical data sheet and presented in Table 14.



Figure 53: AeroMarine silicone product

Table 14: Properties of AeroMarine silicone product

Cost	\$252.00/gallon kit
Specific gravity	1.08
De-mold time [h]	16-24
Pot life [min]	45
Tack-free time [h]	8-12
Useful temperature range [°F]	50-450
Tensile strength [psi]	503

Beeswax is used to fabricate expandable flow channels of the compact heat exchanger. Wax is a recyclable, natural product that can be used in cosmetics, candle making, different polishes, and expandable molds. The melting temperature of beeswax is 65°C, and it is much softer and slightly more flexible in solid phase in comparison to the soy wax. Discoloration of the wax occurs if it is heated above 85°C. Such high temperature can also make it flammable, so any postprocessing of the purchased wax must be conducted carefully. Beeswax melts faster if the melting pots are wider, and it completely hardens in less than 24h at room temperature. It is possible to have it go through multiple melting solidification cycles. The cost of the purchased bees wax was \$7/oz from Amazon.com.



Figure 54: Purchased beeswax (Image courtesy to Amazon.com)

3. Fabrication of expandable flow channels

3.1 Fabrication of the flow channels silicone molds

By using a 3D printed heat exchanger flow channels model discussed in Chapter III, a two-part silicone mold was fabricated. The material used was the silicone mold-making product described in the Materials section of this chapter. The benefits of using silicone molds is because they are reusable, simple to manufacture, and don't produce any toxic waste. Small amount of silicone mixture was poured in a plastic bowl that was previously coated with a lubricant, after which the flow channels model was dipped, and the rest of the silicone mixture was poured over it. Once the silicone was cured, it was removed from the plastic bowl, cut horizontally across the middle so that the 3D flow channels model can be removed. The result was a two-part silicone mold, later used in fabricating expandable flow channels. Any mixture excess was properly disposed. Each mold part weighs ~ 400g and the final results are shown in Figure 55 below.

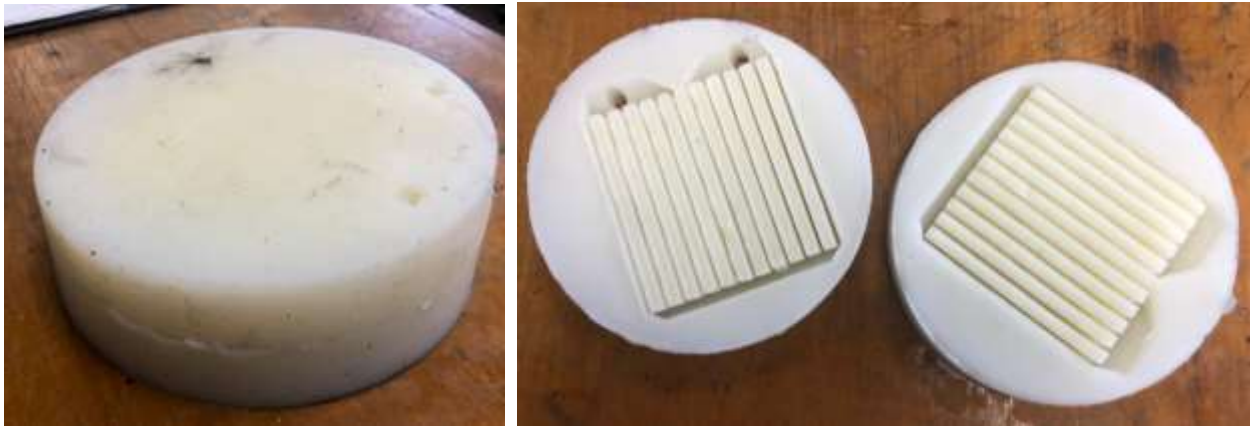


Figure 55: Two-part silicone mold used to manufacture expandable flow channels

3.2 Fabrication of expandable flow channels

Since the goal was to create a flow channel mold that can be easily poured in the mold cavities as well as successfully removed from the polymer heat exchanger (preferably by melting), a natural choice was to start testing out this process by creating wax molds. Previous attempts involved using soy wax, commercially used in making candles. It had similar melting properties as the

beeswax, but it was very brittle once it solidified and would break while separating the silicone molds. Beeswax, on the other hand, is a much softer wax commercially used in cosmetics due to its moisturizing properties and hence was a much better choice for this particular application (we were able to successfully separate silicone molds without damaging the flow channel). The cost difference between the soy wax and the beeswax was negligible, so beeswax was the final material choice for fabricating expandable flow channels.

The beeswax was melted at 80 °C in two wide glass beakers. Wider beakers allowed for a much faster melting process. The silicone mold pieces fabricated in section 4.1 were also placed in the oven for the last 15 minutes of the wax melting process, so that the wax doesn't immediately solidify once it is poured in the mold. Once the molds were taken out of the oven, both pieces were glued with a regular stick glue and reinforced with a Teflon tape. The wax was then slowly poured until the entire mold was filled and it was left to solidify for 24 hours. The flow channels of the solidified wax are not hollow. There is a thin wax layer that has to be manually removed with a scalpel. This process takes about 5 minutes. The wax model can be easily taken from the molds with no damages. Figure 56 shows the resulting flow channels fabricated with the above described method.



Figure 56: Solidified wax flow channels

4. Fabrication of the compact polymer heat exchanger

4.1 Fabrication of the heat exchanger silicone molds

3D printed heat exchanger was used to create another set of silicone molds that will be used for fabricating a compact polymer heat exchanger. The same silicone material was used as previously described in section 3.1. The fabrication method was almost identical, the only difference was that instead of creating two equal silicone pieces, the 3D printed heat exchanger was dipped in the silicone mixture and a thin layer of silicone was poured over it. The top layer was then cut out so that the 3D printed heat exchanger can be taken out. After this mold is prepared, it was important to ensure that the wax flow channels from section 3.2 correctly fit in the newly fabricated silicone mold. It was noted that there is enough clearance between the flow channels and the silicone mold so that the polymer can freely flow around and entirely cover and encapsulate the flow channels. Resulting silicone mold, along with the placed wax flow channel, is shown in Figure 57 below.



Figure 57: Silicone mold for heat exchanger fabrication, with wax flow channels that correctly fit the mold

4.2 Fabrication of the compact polymer heat exchanger

4.2.1 Neat epoxy heat exchanger

A neat epoxy was the first material used in fabricating a compact polymer heat exchanger. A total of 330 gram of the resin + hardener mixture was used. After mechanically mixing resin with hardener, the mixture was degassed for 20 minutes to remove trapped air bubbles. The mixture was then poured over the wax flow channels placed in the heat exchanger silicone mold, shown in Figure 57 ensuring that there is a layer uniformly covering the top surface of the wax mold. The epoxy was cured for 24h at room temperature and taken out of the silicone mold. Once the epoxy was cured, the heat exchanger was placed in the oven at 80 °C to start the wax melting/flow channels removal process. The heat exchanger was turned upside down so that the melted wax can flow out of it.

The process was successful such that the wax was entirely removed from the heat exchanger in ~2.5 hours. However, both bottom and top parts of the heat exchanger had a very thin layer of epoxy (where it touches the silicone mold) that eventually broke and sped up the wax removal process. Furthermore, there were some parts of the uncured epoxy, mainly at the bottom. Further investigation discovered that these issues happened because of the inconsistent clearance between the silicone mold and the wax flow channel walls. This means that the wax flow channels were inclined and raised towards the surface of the heat exchanger, since the amount of epoxy was much heavier than the amount of wax in the silicone mold. Figure 58 illustrates this issue and the resulting wax flow channels removal.



Figure 58: First trial of neat epoxy heat exchanger fabrication- the wax flow channels were entirely removed and there were openings at the bottom of the heat exchanger and by the outlets at the top (marked with black arrows)

Repeated trials still resulted with the same issue where uncured epoxy parts and openings at different locations. Replacing a regular mechanical mixer with a more sophisticated mixer ensured that the resin and hardener are more efficiently mixed, so the issue of uncured epoxy was resolved. It was important to find a way to prevent the flow channels from rising towards the surface and create a support system for them, so additional fabrication steps were implemented. A 4in x 0.5in aluminum plate with two pins of a 0.25in diameter and 1in length was fabricated, shown in Figure 59 below.



Figure 59: Aluminum fixture used to support flow channels mold

The pins of this fixture were inserted in the inlets of the flow channels silicone mold right after the melted wax was poured, as described in section 3.2. The pins were previously coated with a lubricant so that they can easily be removed from the cured wax flow channels, since they need to be taken out of the silicone mold. The buoyancy force on the wax will be countered by the moment on the pins, so the flow channels won't bend or break at the inlets. This fixture-wax mold setup is shown in Figure 60 below.



Figure 60: Fixture-wax mold setup

Once the wax flow channels were placed in the heat exchanger silicone mold, the neat epoxy was poured over and the fixture was placed back. The fixture was removed once the epoxy was entirely cured and the wax melting process was repeated. The result was a neat epoxy heat exchanger with successfully removed wax flow channels, and no openings that occurred in Figure 58. It is evident from Figure 61 that including aluminum fixture in the fabrication procedure helps in leveling the flow channels. Figure 62 shows the fabricated heat exchanger prior to the flow channels removal.

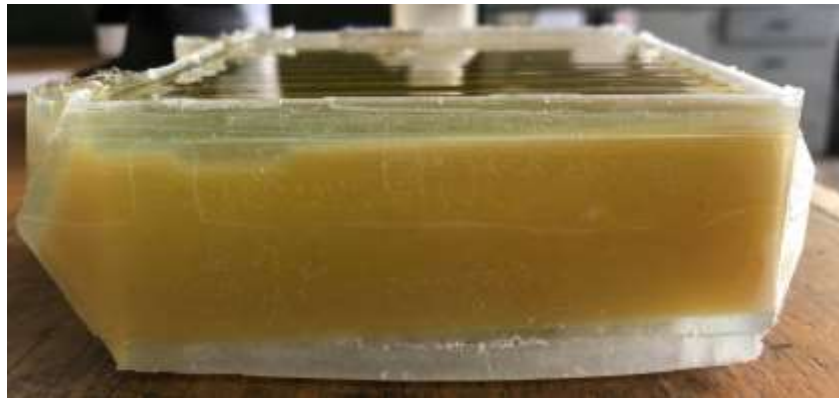


Figure 61: Successful trial of a heat exchanger fabrication after implementing aluminum fixture setup



Figure 62: Compact neat epoxy heat exchanger prior to flow channels removal

Chapter V: Concluding Remarks

1. Results and conclusion

This research is consisted of three main phases- identifying and characterizing material candidates, designing and 3D printing models, and developing a fabrication procedure in order to produce a compact polymer composite heat exchanger. The material candidates considered for the fabrication of a compact polymer heat exchanger included both commercially available materials and composite materials prepared in a laboratory. Each material was characterized for its mechanical, thermal and microstructural properties. TGA and DMA results were conducted in order to determine whether a material would be suitable for prolonged high temperature heat exchanger applications. The results indicated that EPIKOTE™ Resin MGS™ RIMR 135 and EPIKURE™ Curing Agent MGS™ RIMH 137 would be a feasible material candidate since its glass transition temperature is significantly higher than the other two epoxy-based commercial materials, Freeman and Epoxies. In addition, it was found that EPIKOTE™ epoxy has better thermal stability, but its very low thermal conductivity does not make it a suitable material choice as a standalone material. Instead, it was investigated how different thermally conductive additives can enhance thermal conductivity of this polymer.

Copper, graphite flakes and graphene nano powder were selected as reinforcement material candidates because of their much higher thermal conductivities. Cu/epoxy laminates experienced sedimentation due to the weight of the Cu particles. Highest Cu weight percentage, 600%, resulted in densely packed particles, which yielded agglomerations throughout the laminate and significantly increased the overall laminate weight. Furthermore, the use of large amounts of Cu particles is also associated with a substantial cost increase. Laminates containing graphite experienced issues of nonuniform particle distributions due to the higher viscosity at larger weight percentages. Different fabrication methods were tested in order to reduce the laminate viscosity and allow for a more efficient gravity casting. The most successful method was 24h oven cure at 90 °C, pressed between two aluminum plates coated with Teflon® sheets. Different graphite weight percentage laminates were fabricated using this method, as well as the graphite flakes + graphene nano powder hybrid laminates. The main motivation behind adding graphene

nano powder to the graphite flake laminates was that different research groups have proven that the addition of another material creates a better network between the dominating filler material particles and improves structural properties of the laminates. Three-point-bending flexural test results implied that addition of graphene powder would noticeably improve flexural strength of the laminate. However, microstructure analysis shows that both materials do not form a complete structural network, but rather cluster and agglomerate independently. This nonuniform distribution caused the hybrid laminates to have much lower thermal conductivity values compared to the graphite-only laminates. The highest thermal conductivity out of all tested and characterized suitable material candidates was achieved by 35 weight % graphite/epoxy laminate, which was close to 2 W/mK.

Fabricating a compact polymer heat exchanger starts with making 3D models of the heat exchanger and its internal flow channels. The two models were developed so that they can be used in the silicone mold-making process. Silicone has proven to be a good choice for making different molds since it is reusable and will only start tearing down after a very long-time use. The fabricated silicone molds were used to create expandable flow channels and polymer heat exchanger. 3D modeling was evidently a good, affordable and versatile approach in creating both molds since the models can be edited as needed. Expandable flow channels were fabricated by using beeswax, an affordable, non-toxic and reusable material. They were placed in a heat exchanger silicone mold and supported with an aluminum fixture, prior to gravity casting a polymer. The benefit of using gravity casting is that it does not require any sophisticated equipment. It is one of the simplest fabrication methods that was successfully used in fabricating this device. The expandable flow channels were successfully removed by melting the wax once the polymer was cured. Wax has proven to be a great material choice since it allowed for the successful removal of flow channels, and it created a conventional flow channel structure within the cured polymer heat exchanger. The results of all three project phases are promising and can be implemented to fabricate a small-to-medium scale compact heat exchanger with gravity casting using a thermally conductive polymer with a low to medium viscosity.

2. Recommendations for future research

Since graphite seems to be a promising reinforcement material to improve thermal conductivity of a neat epoxy, it should be investigated how different graphite processing methods can be implemented in order to further improve this property. Literature review suggests that different fibers or particle coatings will enhance thermal conductivity of the material, as well as improve structural network of the laminate. It is evident that the increase in graphite weight percentage results in increased thermal conductivity. However, the 600% Cu/epoxy laminates have shown that very large amounts of additives will compromise the quality of the laminate due to particle clustering and sedimentation, as well as increase the overall weight of the laminate. Graphite and hybrid laminates, on the other hand, had a much lower weight percentage, but, based on inspection of the microstructure, still experienced agglomerations and poor particle distribution. Furthermore, this issue affected laminates' mechanical properties, and results indicated that the laminate thickness is not uniform. Therefore, how to improve and control particle dispersion in order to achieve good quality laminates with uniform thickness should be further investigated.

In terms of fabrication, one of the most important issues that should be addressed is viscosity of the polymer, because higher weight percentages of additives drastically increase viscosity of the mixture, which makes gravity casting less efficient. It should be further investigated how different additives or changes in fabrication steps can decrease mixture's viscosity. Conventional heat exchangers have porous space between the flow channel walls in order to increase surface-to-volume ratio and enhance heat transfer. Different ways to achieve this geometry should also be studied. One suggestion is to make a network of dissolvable particles, such as sugar, so that the polymer can flow through the porosities and form a porous geometry after the sugar is removed. This method was tested in our laboratory by fabricating sugar templates that fit between the flow channel walls. These templates were successfully made, but the polymer viscosity was too high for it to entirely flow through. Lastly, a better or more sophisticated fixture that supports wax flow channels and prevents them from floating up may be needed, but the idea of using one should still be applied.

Resolving these issues by implementing new fabrication steps or altering the existing ones would lead to new discoveries and expanding of one's knowledge about polymers, composite materials, importance of material characterizations, and different fabrication methods that exist in the field.

References

- [1] Ahmed T. A. and Kambiz V. “Heat transfer augmentation through convergence angles in a pipe”. *Numerical Heat Transfer, Part A: Applications*, 2017;72:3,197-214.
- [2] El-Dessouky, H. T. and Hisham M. E. “Plastic/compact heat exchangers for single-effect desalination systems”. *Desalination*, 1999;122.2:3,271-289.
- [3] “Compact and Micro-Heat Exchangers”. *Process Intensification*, Elsevier, 2008;77–101
- [4] Githens, R. E. “Flexible-tube heat exchangers”. *Chem. Eng. Prog.*, 1965;61,55-62.
- [5] Hussain, A.R.J, Alahyari, A. A., Eastman, S. A., Thibaud-Erkey, C., Johnston, S. and Sobkowicz, M. J. “Review of polymers for heat exchanger applications: Factors concerning thermal conductivity”. *Applied Thermal Engineering*, 2017;113,1118-1127.
- [6] Chen, X., Yuehong, S., David, R. and Saffa R. “Recent Research Developments in Polymer Heat Exchangers – A Review”. *Renewable and Sustainable Energy Reviews*, 2016;60,1367–1386.
- [7] Bard, S., Schön, F., Demleitner, M. and Altstädt, V. “Copper and Nickel Coating of Carbon Fiber for Thermally and Electrically Conductive Fiber Reinforced Composites”. *Polymers*, 2019;11:5,823.
- [8] Mamunya, Y. P., Davydenko, V. V., Pissis, P. and Lebedev, E. V. “Electrical and thermal conductivity of polymers filled with metal powders”. *European Polymer Journal*, 2002;38:9,1887-1897.
- [9] Xu, Y., Chung, D. D. L. and Mroz, C. “Thermally conducting aluminum nitride polymer-matrix composites”. *Composites Part A: Applied Science and Manufacturing*, 2001;32:12,1749-1757.

- [10] Wang, X., Ho, V., Segalman, R. A. and Cahill, D. G. “Thermal conductivity of high-modulus polymer fibers”. *Macromolecules*, 2013;46:12,4937-4943.
- [11] Mahanta, N. K., Loos, M. R., Zloczower, I. M. and Abramson, A. R. “Graphite–graphene hybrid filler system for high thermal conductivity of epoxy composites”. *Journal of Materials Research*, 2015;30:7,959-966.
- [12] Chen, Y. and Jyh-Ming, T. “Ultra-high thermal conductivity polymer composites”. *Carbon*, 2002;40:3,359-362.
- [13] Cui, W., Du, F., Zhao, J., Zhang, W., Yang, Y., Xie, X. and Mai, Y. W. “Improving Thermal Conductivity While Retaining High Electrical Resistivity of Epoxy Composites by Incorporating Silica-Coated Multi-Walled Carbon Nanotubes”. *Carbon*, 2011;49:2,495–500.
- [14] Fan, Z. and Suresh G. A. “Rheology of Multiwall Carbon Nanotube Suspensions”. *Journal of Rheology*, 2007;51:4,585–604.
- [15] Yue, L., Pircheraghi, G., Monemian, S. A. and Manas-Zloczower, I. “Epoxy Composites with Carbon Nanotubes and Graphene Nanoplatelets – Dispersion and Synergy Effects”. *Carbon*, Elsevier BV, 2014;78,268–278.
- [16] Li, Y., Zhang, H., Porwal, H., Huang, Z., Bilotti, E. and Peijs, T. “Mechanical, Electrical and Thermal Properties of In-Situ Exfoliated Graphene/Epoxy Nanocomposites.” *Composites Part A: Applied Science and Manufacturing*, Elsevier BV, 2017;95,229–236.
- [17] Rogers, T. “Everything You Need to Know About ABS Plastic”. *CreativeMechanisms.com*, 2015